HHS Public Access

Author manuscript

Mol Pharm. Author manuscript; available in PMC 2022 February 07.

Published in final edited form as:

Mol Pharm. 2021 February 01; 18(2): 593–609. doi:10.1021/acs.molpharmaceut.0c00474.

Challenges and Opportunities of Deferoxamine Delivery for Treatment of Alzheimer's Disease, Parkinson's Disease, and Intracerebral Hemorrhage

Amy Corbin Farr,

Department of Pharmaceutical & Biomedical Sciences, College of Pharmacy, University of Georgia, Athens, Georgia 30602, United States

May P. Xiong

Department of Pharmaceutical & Biomedical Sciences, College of Pharmacy, University of Georgia, Athens, Georgia 30602, United States

Abstract

Deferoxamine mesylate (DFO) is an FDA-approved, hexadentate iron chelator routinely used to alleviate systemic iron burden in thalassemia major and sickle cell patients. Iron accumulation in these disease states results from the repeated blood transfusions required to manage these conditions. Iron accumulation has also been implicated in the pathogenesis of Alzheimer's disease (AD), Parkinson's disease (PD), and secondary injury following intracerebral hemorrhage (ICH). Chelation of brain iron is thus a promising therapeutic strategy for improving behavioral outcomes and slowing neurodegeneration in the aforementioned disease states, though the effectiveness of DFO treatment is limited on several accounts. Systemically administered DFO results in nonspecific toxicity at high doses, and the drug's short half-life leads to low patient compliance. Mixed reports of DFO's ability to cross the blood–brain barrier (BBB) also appear in literature. These limitations necessitate novel DFO formulations prior to the drug's widespread use in managing neurodegeneration. Herein, we discuss the various dosing regimens and formulations employed in intranasal (IN) or systemic DFO treatment, as well as the physiological and behavioral outcomes observed in animal models of AD, PD, and ICH. The clinical progress of chelation therapy with DFO in managing neurodegeneration is also evaluated. Finally, the elimination of intranasally administered particles via the glymphatic system and efflux transporters is discussed. Abundant preclinical evidence suggests that intranasal DFO treatment improves memory retention and behavioral outcome in rodent models of AD, PD, and ICH. Several other biochemical and physiological metrics, such as tau phosphorylation, the survival of tyrosine hydroxylase-positive neurons, and infarct volume, are also positively affected by intranasal DFO treatment. However, dosing regimens are inconsistent across studies, and little is known about brain DFO concentration following treatment. Systemic DFO treatment yields similar results, and some complex formulations have been developed to improve permeability across the BBB. However, despite the success in preclinical models, clinical translation is

Corresponding Author May P. Xiong – mpxiong@uga.edu.

The authors declare no competing financial interest.

Complete contact information is available at: https://pubs.acs.org/10.1021/acs.molpharmaceut.0c00474

limited with most clinical evidence investigating DFO treatment in ICH patients, where high-dose treatment has proven dangerous and dosing regimens are not consistent across studies. DFO is a strong drug candidate for managing neurodegeneration in the aging population, but before it can be routinely implemented as a therapeutic agent, dosing regimens must be standardized, and brain DFO content following drug administration must be understood and controlled via novel formulations.

Graphical Abstract

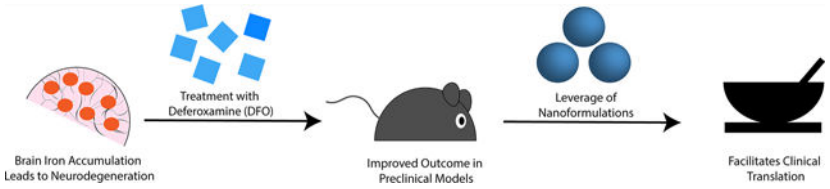

Keywords

deferoxamine; delivery; chelation therapy; neurodegenerative diseases; clinical trials; nanoformulations

INTRODUCTION: THERAPEUTIC EFFICACY AND CLINICAL LIMITATIONS OF DEFEROXAMINE

Deferoxamine mesylate (DFO) is a small molecule iron chelator used to treat acute iron poisoning and chronic iron overload (IO), such as that acquired from frequent blood transfusions in thalassemia major and sickle cell patients.[1] Iron chelators typically contain oxygen, sulfur, and nitrogen atoms.[2,3] Given that iron coordinates six ligands in an octahedral complex, high-affinity iron chelators are generally hexadentate and bind iron in a 1:1 ratio.[1] Iron transport and storage *in vivo* is tightly regulated as exogenous iron mediates organ dysfunction through the production of reactive oxygen species (ROS) via the Fenton reaction.[4–6] Iron accumulation occurs readily in hereditary or diseased conditions as there is no bodily mechanism for the passive excretion of free iron,[6] and DFO provides a means to alleviate iron burden in clinical settings.

Though DFO has great potential to mitigate iron accumulation in clinical settings, its widespread use is limited by adverse side effects. DFO treatment is associated with numerous systemic toxicities, such as toxicity to the cardiovascular, respiratory, gastrointestinal, cutaneous, and nervous systems,[7] as well as ototoxicity, ocular toxicity, and affected renal and liver function at doses greater than 2.5 g per infusion.[8,9] DFO is hepatically metabolized by oxidative deamination.[10] When systemically administered to treat IO patients, such issues can be mitigated by incorporating DFO into macromolecules that prolong circulation time, though these macromolecules must be biodegradable and environmentally responsive to safely promote chelate excretion.[11–13] Ward et al. determined that DFO can cross the blood–brain barrier (BBB) and decrease iron content in both the cerebellum and the cerebral cortex at 30 mg/kg in rats, though other reports suggests that DFO is impermeable to the BBB when compared to other iron chelators and

must be administered in higher doses to be neuroprotective.[14,15] In addition to these concerns, DFO possesses a short half-life (approximately 20–30 min) and patients typically require continuous subcutaneous injections 5–7 days a week, thus resulting in low patient compliance.[8,9] The adverse health effects associated with high doses of systemically administered DFO in tandem with DFO's low patient compliance merit the investigation of alternative means of administration for targeted delivery to the central nervous system (CNS). When DFO was administered intranasally (IN) to seven patients with IO in doses of 0.75–3.0 g, the few side effects observed consisted of mild nasal irritation and a bad taste in the mouth.[16] This report suggests an encouraging alternative for delivering DFO to the CNS to treat Alzheimer's disease (AD), Parkinson's disease (PD), and secondary injury following intracerebral hemorrhage (ICH).

Herein, we review the preclinical and clinical evidence supporting the use of chelation therapy with DFO in treating AD, PD, and secondary injury following ICH. It is noteworthy that iron accumulation is known to contribute to pathogenesis in other neurodegenerative disorders such as Huntington's disease[17,18] and amyotrophic lateral sclerosis (ALS),[19] and that chelation therapy with DFO has shown efficacy in animal models of these neurodegenerative disorders,[20,21] though such evidence is not within the scope of this article. In addition to the preclinical and clinical progress of chelation therapy with DFO in treating AD, PD, and secondary injury following ICH, we also discuss progress in the development of sophisticated nanoformulations of DFO designed to treat these conditions, with an emphasis on IN delivery, and highlight the necessity for such nanoformulations based on the limitations presented above. The mechanism and challenges associated with IN delivery are briefly discussed, and conclusions and perspectives for the field are suggested.

MECHANISMS OF NOSE-TO-BRAIN DELIVERY AND THE ASSOCIATED CHALLENGES

Nose-to-brain transport via IN administration is a promising alternative to systemic administration as this method bypasses the BBB and first-pass metabolism, results in the rapid onset of therapeutic effect, improves drug concentration in the brain, reduces systemic side effects, and is minimally invasive to patients.[22–24] Direct nose-to-brain transport can occur along the olfactory nerve pathway and the trigeminal nerve pathway.[22,25–27] The olfactory region of the nasal cavity is located on the superior aspect and is connected to the olfactory bulb of the brain via olfactory nerves.[25] The middle region of the nasal cavity, the respiratory region, is innervated by the trigeminal nerve, which originates in the pons of the brain-stem.[25] The trigeminal nerve also innervates the olfactory region.[22,28] The respiratory region has a very large surface area, ~130 cm^2, and is highly vascularized.[29,30] Due to this high vascularity, a significant portion of the drug that reaches the respiratory region enters the bloodstream and is circulated systemically.[25] Though drugs absorbed into the bloodstream may enter the brain through the BBB, this constitutes a minor pathway.[25] IN administered drugs can be dispersed throughout the brain following direct neuronal transport via the olfactory and trigeminal nerves, and such transport can occur via both intracellular and extracellular pathways.[31] The intracellular pathway begins with internalization via pinocytosis or receptor-mediated endocytosis to a lesser extent, and the

resulting endosomes are subsequently trafficked along the axon.[25] Neuronal translocation is a slow process due to diffusion within the nasal cavity, endocytosis at the membrane, Golgi vesicle trafficking, and vesicle binding prior to exocytosis at the nerve terminal.[25] In the extracellular pathway, administered drugs cross olfactory or respiratory epithelium and diffuse through tight junctions in the paracellular space.[25] Small, hydrophilic drugs are more likely to enter the brain by this mechanism, and this mechanism is significantly faster than its intracellular counterpart.[32]

Despite the great potential of this strategy, several factors of nasal physiology present challenges to IN drug delivery. Mucociliary clearance (MCC) results in the transport of mucous to the nasopharynx, where it is swallowed and ultimately deposited in the gastrointestinal tract.[23,33,28] This process occurs every 15–20 min.[23,34] In this process, particulate degree entrapped in mucus is cleared by the “conveyor belt mechanism” of beating cilia.[34] Increased production of mucus or a decrease in mucus viscosity may result in an increased rate of MCC.[34] The nasal epithelium is also rich in degradative enzymes such as carboxyl esterases, aldehyde dehydrogenases, epoxide hydrolases, cytochrome P450 isoenzymes, and various proteolytic enzymes, thus the need for novel IN formulations capable of increasing mucoadhesion and protecting drugs against degradation.[34] As a result of such physiology, drugs administered IN often demonstrate poor retention time and inadequate permeation across the membrane, thus limiting bioavailability following administration. Drug physicochemical properties such as molecular weight, pK_a, and hydrophilicity also significantly impact nasal absorption, as does formulation viscosity, pH, and composition.[34] Notably, certain pharmaceutical excipients are known to cause nasal irritation, which may result in decreased patient compliance.[34] To combat the challenges associated with nasal physiology, various nanoparticle and microparticle formulations containing prodrugs, mucoadhesive polymers, absorption enhancers, and enzymatic inhibitors have been developed to improve nasal drug absorption.[34]

ALZHEIMER’S DISEASE

Impact of Iron Accumulation.

AD is a neurodegenerative condition frequently observed in the elderly population that results in memory loss, language disorders, loss of directionality, and anxious behavior as well as impaired bodily function and mental cognition in late-stage patients.[35–37] From a histopathological standpoint, AD is characterized by senile plaques (SP) formed from the deposition of extracellular β-amyloid (Aβ) protein and neurofibrillary tangles (NFTs) resulting from the hyperphosphorylation of the tau proteins of neuronal microtubules.[36] Brain iron content has been found to increase with age, and MRI confirms a more significant increase in iron content in the brains of AD patients.[39] Experimental evidence indicates elevated levels of zinc, copper, and iron in SP of AD patients, and it is suggested that trace metals may increase β-amyloid protein aggregation and SP toxicity by generating free radicals.[40,41] β-Amyloid protein binds and stabilizes iron ions through three histidine residues and one tyrosine residue, which reduces the peptide’s helix structure and increases β sheet content, thus enhancing peptide–peptide interaction and increasing fibril formation.[42–44] Aβ42 does not form β-pleated amyloid when incubated with DFO

in vitro in the presence or absence of aluminum or iron.[45] In the post-mortem studies of 10 AD patients, iron was stripped from the NFTs of fixed hippocampal tissue at room temperature after 20 min exposure to 0.1 M DFO, though a 15 h incubation was required to strip iron bound to SP.[46] DFO has also been observed to protect against lipopolysaccharide (LPS)-induced neuroinflammation and the associated cognitive deficits in adult mice when administered intracerebroventricularly.[47]

Preclinical Studies of IN DFO.

IN delivery of DFO consistently decreases memory loss, improves spatial learning, and corrects for altered behavior when administered to AD models of mice and rats at various doses and dosing intervals (Table 1). Increased expression and phosphorylation of amyloid precursor protein 695 (APP695), increased amyloidogenic APP cleavage, increased Aβ deposition, and thus impaired spatial learning and memory were observed when transgenic mice expressing presenilin-1 (PS1) and APP were watered with high-dose iron.[48] IN administration of 200 mg/kg DFO every other day for 90 days reversed the aforementioned behavioral alterations by shifting APP processing to a nonamyloidogenic pathway, consequently reducing the Aβ burden.[48] When administered to APP/PS1 amyloid mice from 36 to 54 weeks of age (3 times per week for 18 weeks), chronic low dose IN DFO decreased the loss of reference and working memory in Morris and radial arm water mazes, decreased soluble Aβ40 and Aβ42 deposition in the cortex and hippocampus, and decreased the activity of glycogen synthase kinase 3β (GSK3β), resulting in lower oxidative stress and impacting several targets implicated in the neuropathology of AD.[49] Further research has confirmed that high-dose iron treatment increases tau phosphorylation at the Thr205, Thr231, and Ser396 sites, thus facilitating NFT formation in double transgenic mice, though this induced hyperphosphorylation is significantly reduced by IN DFO administration as DFO decreases the activity of iron-induced cyclin-dependent kinase 5 (CDK5) and GSK3β.[50] Interestingly, IN DFO administration was found to inhibit tau phosphorylation at only the Ser396 site.[50] In APP/PS1 mice, IN DFO has also been found to upregulate the P38/HIF-1α pathway and multiple proteins encoded by HIF-1-dependent neuroprotective-adaptive genes, such as transferrin receptor (TFR), divalent metal transporter 1 (DMT1), and brain-derived neurotrophic factor (BDNF).[51] Iron chelation is thought to stabilize the transcriptional complex HIF-1 and activate a signal transduction pathway for hypoxic adaptation.[52–54]

Similarly, when P301L mice exhibiting hyperphosphorylated tau accumulation were treated with 2.4 mg of IN DFO three times a week for five months, TG-DFO mice performed comparably to WT mice in radial arm water maze behavioral testing, while the performance of TG-saline mice was considerably worse.[55] P301L transgenic mice also exhibited significantly lower pGSK3β and HIF-1α levels than WT mice, and treatment with DFO reduced these differences, though no significant decrease in phosphorylated tau was observed in the brain tissue of DFO-treated mice.[55] IN DFO has also been found to improve outcome in intracerebroventricular streptozotocin (ICV STZ) rat models of sporadic AD, which differ from the aforementioned models in that they exhibit irregular insulin metabolism in addition to oxidative stress.[56] ICV STZ rats treated with IN DFO both pre- and post-surgery demonstrated shorter escape latencies in spatial memory tests with

the Morris water maze, while pre-treatment decreased foot slips on the tapered balance beam test.[56] Additionally, brain tissue analysis revealed decreased oxidative stress, greater insulin receptor expression levels, and decreased ratio of pGSK3β/GSK3β in ICV STZ rats pre-treated with DFO compared to sham-saline and post-treated STZ-DFO rats.[56]

Hanson et al. reported that IN DFO reaches detectable concentrations in all areas of the CNS.[57] The largest concentrations of DFO were recorded in the olfactory bulb and trigeminal nerve, which are the proposed pathways for IN drug delivery to the brain.[57] IN DFO resulted in limited systemic exposure (8.5 μM in the kidneys and 5.2 μM in the blood).[57] Hanson et al. also observed improved performance in the Morris water maze and reduced brain aluminum concentrations in IN DFO-treated APP/PS1 mice when compared to transgenic mice receiving vehicle.[57]

Preclinical Studies of Systemic DFO.

Systemically administered DFO also demonstrates therapeutic potential in various animal models of AD (Table 2). Aluminum has been suggested as a causal agent in AD pathogenesis given its deposition in NFTs, determined via laser microprobe mass analysis, and epidemiological studies of drinking water.[58] Intracisternal injection of aluminum maltolate to New Zealand white rabbits modeled AD by inducing neurofibrillary degeneration in neuronal cell bodies and brain and spinal cord neurites.[59] When administered 2 days prior to sacrifice on day 4, 6, or 8, intramuscular (IM) DFO injections reduced the number of NFT-positive neurons in aluminum-treated rabbits as quantified by tau monoclonal antibody staining.[59]

Chronic oral exposure (6 months) to aluminum in female amyloid beta peptide (AβPP) transgenic mice also models AD.[60] When these mice received subcutaneous (SC) DFO treatment (0.20 mmol/kg/day twice per week for 6 months beginning at 5 months of age), a direct correlation between the overexpression of antioxidant enzyme mRNA and DFO treatment was not observed, so experimental evidence did not indicate that DFO treatment aids in preventing prooxidant events.[60]

Clinical Studies of IN and Systemic DFO.

According to Agrawal et al., PubMed and clinicaltrials.gov, no clinical studies investigating the therapeutic benefit of IN DFO in AD patients have been conducted to date.[61] However, a two-year, single-blind clinical study in 1991 found that IM administered DFO (125 mg twice a day, 5 days per week) reduced the rate of decline of daily living skills in DFO-treated AD patients by half when compared to a group treated with an oral placebo and a no-treatment group, thus suggesting that IM DFO slows the progression of AD (Table 3).[62] Weight loss and loss of appetite have been observed as side effects in DFO-treated patients, along with the increased formation of a monoamine oxidase catalyzed metabolite, MF01.[62,63] Disease progression has also been monitored with a videotaped home behavior instrument with strong criterion references over the course of two years, and trace metal analysis of autopsied brain tissue indicated that DFO-treated patients had neocortical aluminum concentrations similar to the control group.[64] An actively recruiting Phase II randomized, multicenter, double-blind, placebo-controlled clinical trial investigating the

safety and efficacy of 600 mg delayed-release deferiprone oral tablets in slowing dementia progression in prodromal AD and mild AD patients is in progress (ClinicalTrials.gov Identifier: NCT03234686).

PARKINSON'S DISEASE

Impact of Iron Accumulation.

PD is a progressive neurodegenerative disorder that manifests as tremors, rigidity, and bradykinesia and is characterized by the loss of dopaminergic neurons in the substantia nigra (SN) and subsequent dopamine depletion in the striatum.[65,66] Though the mechanism of pathogenesis is not well-understood, iron accumulation in dopaminergic and glial cells of the SN has been observed in PD animal models as well as post-mortem brains, and the severity of motor symptoms in PD patients parallels iron levels in the SN.[67–70] Iron is thought to contribute to dopaminergic cell death by catalyzing the production of ROS from hydrogen peroxide, a byproduct of dopamine catabolism, thus resulting in oxidative stress, lipid peroxidation, and membrane fluidity.[15,71] Brain-permeable iron chelators have been shown to inhibit iron-induced lipid peroxidation when injected intraventricularly and intraperitoneally (IP) in rats, thus reinforcing the role of iron in PD pathogenesis.[15]

Preclinical Studies of IN DFO.

IN DFO has also demonstrated neuroprotective effects in animal models of PD (Table 4). PD can be induced in rats via a unilateral injection of 6-hydroxydopamine (6-OHDA) into the medial forebrain bundle.[72] Pre-treatment with IN DFO in the 4 days prior to 6-OHDA injection and post-treatment twice a week for one month after injection resulted in a decreased number of contralateral turns in an apomorphine-induced rotational test, decreased limb asymmetry, and increased preservation of tyrosine hydroxylase immunoreactive neurons in the SN of IN DFO rats when compared to rats that received IN saline.[72] Neurodegeneration of dopaminergic neurons can also be induced via injection of 1-methyl-4-phenyl-1,2,3,6-tetrahydropyridine (MPTP).[73] IN DFO administered every other day for 4 weeks (200 mg/kg dose) following MPTP injection effectively increased the survival of tyrosine hydroxylase-containing neurons, decreased the activity of astrocytes in the SN and striatum, alleviated motor defects in an open field test, and upregulated HIF-1α protein, tyrosine hydroxylase, vascular endothelial growth factor (VEGF), and growth-associated protein 43 (GAP43).[73] IN DFO treatment also downregulated α-synuclein, DMT1, and transferrin receptor (TFR) by inhibiting the phosphorylation of c-Jun N-terminal kinase (JNK) and inducing the phosphorylation of extracellular regulated protein kinases (ERK) and mitogen-activated protein kinase (MAPK)/P38 kinase.[73] Unilateral injection of a recombinant adeno-associated viral vector (rAAV) encoding α-synuclein to rat midbrain also produces a PD model.[74] When α-synuclein rat models were treated 3 times per week with 6 mg doses of IN DFO for either 3 or 7 weeks beginning 1 week after surgery, data indicated a decrease in α-synuclein accumulation in striatal fibers at the terminal level and partial improvement in motor behavior in stepping tests, drug-induced rotational tests, and cylinder tests, though IN DFO did not protect against dopaminergic cell death in this time frame or dosage.[74] IN DFO also decreased early VMAT2+ accumulation but did not stop its incorporation over time.[74]

Preclinical Studies of Systemic DFO.

Systemic administration of DFO has also been proven to slow disease progression in animal models of PD (Table 5). When administered systemically to the 6-OHDA rat model previously described, DFO (30 mg/kg), deferiprone (10 mg/kg), and desferasirox (20 mg/kg) attenuated the loss of dopaminergic neurons and striatal dopamine content, and when used in pretreatment via a microdialysis probe into the striatum, prevented the generation of hydroxyl radicals.[75]

When administered IP at 30 mg/kg 3 times per week for 2 weeks, DFO decreased brain iron content in the cerebellum and cerebral cortex of ferrocene-loaded rats, thus altering dopamine metabolism by reducing dopamine turnover and DOPAC, a dopamine metabolite, 2 and 4 weeks after treatment.[14] IP administration of DFO (60 mg/kg/day) to rotenone-induced PD male Wistar rats inhibited iron deposition in the SN, the striatum globus pallidus, the hippocampus, and the cerebellum and reduced the loss of tyrosine hydroxylase-positive cells.[76] Similarly, IP DFO (50 mg/kg) prevented the loss of dopaminergic neurons and maintained striatal dopamine levels in the 6-OHDA PD model.[77] Following an identical dosing regimen, Lv et al. found that combined treatment with DFO and curcumin amplified the neuroprotective effects of DFO in 6-OHDA Sprague–Dawley rats.[78] Curcumin is a polyphenolic pharmaceutical agent that possesses anti-inflammatory, anti-oxidant, anti-proliferative, and anti-angiogenic properties.[79]

Clinical Studies of IN and Systemic DFO.

Per clinicaltrials.gov, Google Scholar, and PubMed, at the time of this review, no clinical trials investigating the effects of DFO treatment on outcome in PD patients have been conducted. However, a translational study employing mitochondria from both peripheral blood mononuclear cells from PD patients and human mesencephalic dopaminergic cells and an MPTP mouse model found that deferiprone reduced labile iron in the mitochondria and induced cryoprotection and available dopamine content in the mouse model more profoundly than DFO.[80] A double-blind, randomized, placebo-controlled Phase II clinical trial indicated that the oral administration of deferiprone (30 mg/kg/day in two doses) improved motor signs at 6 months and decreased handicap and IO at 1 year in 40 early-stage PD patients (within four years of onset) (ClinicalTrials.gov: NCT00943748).[80] Numerous clinical trials evaluating the efficacy and safety of deferiprone in the treatment of PD, including dose-ranging studies, *ex vivo* studies of PD patient peripheral blood mononuclear cells and platelets, and conservative iron chelation studies, reiterate the benefits of chelation therapy in treating neurodegenerative diseases (ClinicalTrials.gov Identifiers: NCT02728843, NCT02880033, NCT00943748, NCT02655315, NCT01539837).[81–83]

INTRACEREBRAL HEMORRHAGE

Impact of Iron Accumulation.

ICH is a subtype of stroke resulting from the rupture of blood vessels in the brain.[84,85] ICH accounts for 10–15% of strokes worldwide and is often correlated to inadequate control of blood pressure and the overprescription of anticoagulants, thrombolytics, and antiplatelet agents.[84,86] Experimental evidence suggests that hemoglobin is a mediator of

neurotoxicity when injected into the brain *in vivo* or added to cultured neurons *in vitro*.[87] Hemorrhaged blood is rich in hemoproteins that release biliverdin, carbon monoxide, and free iron upon breakdown by heme oxygenase.[85] Iron toxicity results from free radical production via the Fenton reaction, and oxidative stress causes mitochondrial fragmentation in hippocampal neurons, perihematomal edema, and ultimately, glial and neuronal cell death.[88] When administered to anesthetized felines and Sprague–Dawley rats, hemoglobin inhibits Na/K ATPase and catalyzes lipid peroxidation in CNS homogenates by hydroxyl radical formation, thus promoting delayed edema formation and secondary neuronal injury after ICH upon the lysis of red blood cells (RBCs).[89,90]

Preclinical Studies of IN DFO.

Preliminary experimental evidence suggests that IN DFO demonstrates neuroprotective effects following stroke in an ischemic stroke rat model (Table 6). Most notably, Hanson et al. reported that when administered IN, a 6 mg dose of DFO resulted in a brain concentration of 0.9–18.5 μM after 30 min, where brain concentration at the same time interval was 0.1–0.5 μM following IV administration in rat models of middle cerebral artery occlusion (MCAO).[91] Both pre-treatment (three 6 mg doses 48 h prior to MCAO) and post-treatment (six 6 mg doses immediately after reperfusion) with IN DFO decreased infarct volume by 55% relative to the control.[91]

Preclinical Studies of Systemic DFO.

Abundant preclinical evidence supports DFO as a candidate in the treatment of secondary injury following ICH. Cui et al. reported that in 20 unique studies, DFO reduced brain water content by 85.7% and improved neurobehavioral score by –1.08 in various animal models of ICH, though additional confirmation may be necessary due to poor study quality and publication bias.[92] The same body of evidence also indicated that DFO is most effective when administered 2–4 h after ICH at a dose of 10–50 mg/kg via the IM and IP routes.[92] DFO facilitates neuroprotection after injury through an antioxidative mechanism and neurorepair via HIF-1α activation in both ICH and ischemic stroke.[93] IM DFO decreases ICH-induced perihematomal iron accumulation, neuronal injury, perihematomal white matter edema, and tumor necrosis factor-$\mu\alpha$ (TNF-$\mu\alpha$) and receptor-interacting protein kinase 1 (RIPK1) levels in the brains of piglet models of ICH.[94,95] Activation of the death-domain receptor RIPK1 by TNF-$\mu\alpha$ contributes to necroptosis, a nonapoptotic cell-death pathway observed in delayed neuronal injury.[96] Tabular data for this topic is provided in the aforementioned review.

Clinical Studies of IN and Systemic DFO.

Zeng et al. recently reviewed clinical studies of DFO intervention after ICH, though the two reports highlighted are of small sample size and are therefore not conclusive in determining the safety or effectiveness of DFO intervention in neurological outcome.[97] Yu et al. reports that IV DFO intervention (32 mg/kg/day for 3 days, where the infusion rate did not exceed 7.5 mg/kg/hour and 6000 mg/day was the maximum dose regardless of patient weight) reduced relative edema volume and hematoma absorption after 15 days of treatment, though no significant differences in neurological scores were observed between the control and treatment groups after 15 and 30 days. This clinical study was randomized, controlled, and

had 42 participants.[98] Wu et al. reports a similar outcome: when 29 participants were treated with 20 mg/kg/day of IV DFO for 3 consecutive days after the first admission, the control group's relative edema volume was higher at days 7 and 14, and the treatment group had a better neurological function at these checkpoints than did the control group.[97] However, no significant difference in neurological function was observed between the two groups after 90 days, as consistent with the aforementioned clinical study.[97]Tabular data for this topic is provided in the aforementioned review.

An open-label Phase I study indicated that IV DFO is safe at a maximum tolerated dose (MTD) of 62 mg/kg/day up to 6000 mg/day without any serious adverse events (SAEs) or increased mortality.[99] DFO also has modest effects in reducing blood pressure, and clinical evidence supports that the reduction of blood pressure in ICH patients is not only safe but may reduce neurological deterioration if done aggressively in the first 24 h.[100] A multicenter, double-blind, Phase II clinical trial in which 324 patients exhibiting spontaneous ICH were randomized and treated with either IV DFO (62 mg/kg/day for 5 consecutive days) or a saline placebo was conducted to access the feasibility of high-dose IV DFO administration in Phase III Clinical Trials (ClinicalTrials.gov Identifier: NCT01662895).[101] The aforementioned study was terminated due to an increased incidence of acute respiratory distress syndrome (ARDS) (ClinicalTrials.gov Identifier: NCT01662895).

DFO has also been found to accelerate hematoma absorption and inhibit edema formation after isolated traumatic ICH.[102] Patients were admitted within 8 h of incident, and those in the experimental group were given 20 mg/kg/day of IV DFO for 5 days.[102]There was no significant difference in hematoma volume after 2 weeks, though hematoma volume decreased more rapidly in the experimental group.[102] It is noteworthy that the assignment of patients to the experimental and control groups was nonrandom and 94 patients were used in the final analysis after propensity-score matching analysis; an attending neurosurgeon classified patients, though no rationale is given for classification.[102]

In 2019, a multicenter, double-blind, placebo-controlled Phase II clinical trial with 294 participants found that IV DFO treatment (32 mg/kg/day for 3 consecutive days) was safe and did not result in treatment-related deaths or SAEs (Clinical-Trials.gov Identifier: NCT02175225).[103] Good clinical outcome, the primary outcome, was measured via a modified Rankin scale score of 0–2 after 90 days.[103] However, a futility analysis at the 90% upper confidence bound indicated that in a Phase III clinical trial, IV DFO treatment at this dose and dosing interval would not significantly improve good clinical outcome at 90 days.[103]

In addition to these studies, a distinct Phase I dose-finding and safety study of DFO in 20 ICH patients was marked completed as of January 2018, though no data was linked to the identifier as of May 2019 (ClinicalTrials.gov Identifier: NCT00598572). Various dosing regimens, 7 mg/kg to 125 mg/kg, were tested in cohorts of 3 subjects. The maximum allowable dose was 6000 mg/day regardless of patient weight. An actively recruiting, randomized Phase I clinical trial evaluating the efficacy and safety of DFO treatment for ICH is in progress as of May 2019 (ClinicalTrials.gov Identifier: NCT02367248). The

treatment regimen entails a continuous IV infusion of DFO in 20 mL of sterile water (40 mg/kg/day up to 6000 mg/day) for 5 consecutive days beginning 12 h after the onset of symptoms. In the study, DFO is an active comparator to the Phase II drug Xingnaojing, a traditional Chinese medicine consisting of four Chinese herbs.[104]

IN NANOFORMULATIONS OF DFO

Alzheimer's Disease.

Though no IN nanoformulations of DFO or other iron chelators have been designed specifically to treat AD, IN nanoformulations of DFO that are broadly designated to treat neurodegeneration have been reported. For example, Rassu et al. has investigated means of increasing the nose-to-brain transport of DFO through solid formulations based on the absorption enhancers chitosan and methyl-β-cyclodextrin.[105] Cyclodextrins form inclusion complexes with membrane lipids such as cholesterol, sphingomyelin, and phosphatidylcholine to compromise membrane integrity and decrease rigidity, while chitosan reversibly opens tight junctions and absorbs water from the mucus layer to form a gel-like layer along the epithelium and improve bioavailability.[106,107] *In vitro*, methyl-β-cyclodextrin microparticles increased DFO permeation across lipophilic membranes and a monolayer of neuron-like PC 12 cells relative to chitosan-based formulations, though neither formulation improved DFO permeation across epithelial-like Caco-2 monolayers.[105] Additionally, IN administration of a 200 μg dose of DFO encapsulated in these microparticles resulted in uptake to the cerebrospinal fluid 30 min after insufflation, with systemic absolute bioavailability of 6% and 15% for chitosan and methyl-β-cyclodextrin, respectively.[105] No uptake was observed for DFO in a water solution.[105] Other examples of the efficacy of β-cyclodextrin-mediated IN drug delivery have been reported. Thermally cross-linked bovine serum albumin nanoparticles carrying β-cyclodextrin or its hydrophilic derivatives (hydroxypropyl β-cyclodextrin and sulphobutylether β-cyclodextrin) loaded by soaking with the cholinesterase inhibitor Tacrine demonstrated increased mucoadhesion and sustained drug release over the course of 400 min *in vitro*.[108] Ex vivo permeation studies also indicated that cyclodextrin-containing albumin nanoparticles demonstrated increased permeation across sheep nasal mucosa than albumin nanoparticles alone.[108] It is noteworthy that ethanol was employed in the coacervation of albumin as opposed to acetone as acetone can damage nasal mucosa in millimolar concentrations.[109]

Though IN and systemic nanochelator formulations are limited in the context of AD, the use of nanotechnology in treating this condition has been explored extensively. Agrawal et al. has reviewed the use of surface-modified liposomes[110] and other nanotechnologies such as nanogels, nanodispersions, lipid-based systems, nanoemulsions, and other nanoparticles designed to permeate the BBB,[111] along with liposomal technologies for IN delivery.[110] A few notable IN delivery strategies are summarized here. Ionically cross-linked piperine (PIP)-loaded chitosan (CS)/tripolyphosphate (TPP) nanoparticles have proved efficacious in the treatment of AD when IN administered.[112] Nanoparticles loaded with the alkaloid phytopharmaceutical PIP demonstrated both an antioxidant effect and Ach esterase inhibition in rat models of AD (ICV injection of colchicine) without brain toxicity or nasal irritation.[112] The IN dose was 20-fold less than the previously employed oral

dose, which displayed hydrophobicity and extensive presystemic metabolism.[112] PEG-surface-modified liposomes containing the peptide H102, a β sheet breaker designed to specifically bind the monomer A$\beta_{1–42}$ and prevent its misfolding and aggregation, have also been effective in penetrating human airway serous Calu-3 cell line monolayers *in vitro* and ameliorating spatial memory impairment, increasing the activity of ChAT and inhibiting senile plaque formation in rat models of AD (bilateral injection of A$\beta_{1–40}$ into hippocampus) when compared to IN H102 solution containing 1% chitosan absorption enhancer.[113] Similarly, radioactive tracing with the encapsulated ^{125}I-labeled basic fibroblast growth factor (bFGF) following IN administration of Solanum tuberosum lectin (STL) conjugated poly(ethylene glycol)-poly(lactic-co-glycolic acid) (PEG-PLGA) nanoparticles to β-amyloid$_{25–35}$ rat models of AD revealed greater concentration in the olfactory bulb, cerebellum, and cerebrum as well as the increased neuroprotective effect of bFGF in comparison to IN solution and unmodified nanoparticles. Histopathology assays did not indicate safety issues or immunogenic responses from the STL-bFGF-NP.[114]

Parkinson's Disease.

A few examples of systemic nanoformulations of DFO designed to treat PD have been reported, though IN nanochelator formulations remain limited. To promote delivery across the BBB, DFO was encapsulated in the hydrophilic core of methoxypoly(ethylene glycol)-poly-(lactic-co-glycolic acid) (mPEG–PLGA) amphiphilic copolymers, and this core nanoparticle was then conjugated to the brain-targeting peptide rabies virus glycoprotein (RVG) 29, which is proposed to trigger specific receptor-mediated endocytosis at the extracellular surface of brain microvascular endothelial cells and neurons.[115] When administered to MPTP-induced PD mice at 35 mg/kg IV once every other day for 12 days following MPTP injection, RVG29-DFO mice stayed longer on a rotating rod than PD mice, free DFO mice, and mice treated with mPEG–PLGA-DFO.[115] RVG29-DFO-treated mice also demonstrated reduced loss of tyrosine hydroxylase-positive neurons.[115]

Lipophilic conjugates of DFO have also been evaluated for therapeutic potential in an MPTP mouse model of PD as they are more permeable with respect to the BBB.[116] The hydrophobicity of DFO was increased by conjugating the following ancillary antioxidant compounds to the amine terminus: a truncated Vitamin E variant, carboxylic acid derivatives of edaravone, and a methylated derivative of 3-(6-hydroxy-2-methylchroman-2-yl)propionic acid.[116] In addition to an added antioxidant mechanism facilitated by the ancillary group, the lipophilic conjugates showed increased plasma protein binding and a statistically significant increase in neuronal cell counts and motor function when administered to MPTP mouse models of PD.[116] Liddell et al. observed similar results *in vitro*, where lipophilic DFO analogs produced via conjugation to adamantane derivatives or deferasirox improved outcome in numerous cell lines.[117]

Mursaleen et al. evaluated the *in vitro* efficacy of nanoformulations combining DFO and the antioxidant Curcumin in combatting oxidative stress and rotenone-induced decreases in cell viability in SH-SY5Y cells.[118] When Curcumin and DFO were combined in Pluronic F68 nanocarriers with dequilinium, a mitochondrial targeting agent, viability increased up to 10%, and all nanoformulations of DFO or Curcumin with or without dequilinium

prevented lipid peroxidation. Though an *in vivo* model was not employed, this approach demonstrates the utility of antioxidant and iron-chelating drugs when used in combination to treat disorders of the CNS.

The various IN and systemic nanotechnologies that have been leveraged to treat PD have been extensively reviewed,[119–121] so only a few studies will be reiterated here. A nanoparticle employing non-Fe hemin as the iron chelator and protected by a zwitterionic species was conjugated to HIV-1 trans-activating transcriptor (TAT) to promote delivery across the BBB.[122] Though this formulation does not incorporate DFO, it enhanced chelator lifetime and alleviated both physiological and behavioral deficits in Parkinsonian mice, thus reinforcing the potential of chelation therapy in treating PD and providing a useful strategy to promote BBB permeability. Odorranalectin (OL), a small lectin capable of binding the sugar L-fucose on the olfactory epithelium of the glycosylated nasal mucosa, has also been leveraged.[123,124] When OL was conjugated to PEG-PLGA nanoparticles and the tracer DiR encapsulated, *in vivo* fluorescence imaging revealed greater fluorescence intensity in the brains of mice administered OL nanoparticles than mice treated with unmodified nanoparticles.[124] Additionally, OL nanoparticles containing the macromolecular drug urocortin peptide (UCN) demonstrated improved therapeutic efficacy in 6-OHDA-induced hemiparkinsonian rats in apomorphine-induced rotation behavior tests, neurotransmitter determination, and tyrosine hydroxylase tests when compared to unmodified nanoparticles and UCN solution.[124] Unlike wheat germ agglutinin (WGA) and other large lectin members that improve brain delivery of peptide-loaded nanoparticles, OL is advantageous in that it is less immunogenic due to its relatively low molecular weight.[124–127] Though this nanoparticle has not been investigated in tandem with chelation therapy, it represents an interesting avenue for potential exploration.

Intracerebral Hemorrhage.

IN and systemic nanochelator formulations of DFO for ICH have yet to be explored in the literature, though a novel carbon nanoparticle formulation has been used to deliver DFO IP following induced ICH.[128] In this report, highly oxidized hydrophilic carbon clusters (HCCs) were PEGylated and loaded with DFO. DFO loading onto the nanoparticle was calculated via thermogravimetric analysis. PEG-HCCs demonstrate antioxidative properties by mimicking superoxide dismutase activity. *In vitro*, PEG-HCCs decreased the accumulation of ROS and damage to both nuclear and mitochondrial DNA and also partially attenuated cell death in hemin-treated cultures. DFO-PEG-HCC multifunctional nanoparticles decreased DNA damage markers compared to DFO or PEG-HCC treatment alone, and DFO-PEG-HCCs prevented senescence and ferroptosis *in vitro*. When administered IP to a C57BL/6 mouse model 30 min after ICH was induced, DFO-PEG-HCCs attenuated genomic damage in both the nucleus and mitochondria and decreased senesce markers compared to untreated ICH controls. ICH was induced by injecting blood lysed via freeze–thawing to maximize exposure to blood components. The data from this study suggests that when used in combination, antioxidative and iron-chelating therapeutics may improve outcome following ICH. The various nanochelators designed to treat AD, PD, and ICH that have been evaluated *in vivo* are tabulated in Table 7.

Other Nanoformulations of DFO.

Numerous transfusional nanoformulations of DFO have been developed to improve patient compliance in the treatment of secondary IO resulting from the repeated blood transfusions necessary to combat hemochromatosis and hemoglobinopathies. In a recent review, Jones et al. highlighted the use of polymeric materials, dendrimers, polyrotaxanes, micelles, nanogels, liposomes, and nanoparticles in fabricating nanochelators that increase circulation time and mitigate adverse effects.[129] Many natural and synthetic materials have been leveraged in both conjugation and controlled release strategies. For instance, DFO has been conjugated to starch, polylysine, and polyrotaxane polymers as well as hyper-branched polyglycerol dendrimers and acrylate-based nanogels to increase half-life while promoting elimination *in vivo*. In the way of controlled release, mPEG–PLGA nanoparticles and phosphatidyl choline cholesterol liposomes have been used to encapsulate DFO and show promising results in mouse models.[129] However, while nanochelators hold tremendous potential in treating IO, the authors note that more standardized approaches are required to accurately evaluate clinical potential.[129]

Transdermal nanoformulations of DFO have also been reported to treat ulcers and accelerate skin wound healing. For example, reverse micelles encapsulating polyvinylpyrrolidone (PVP)-DFO aggregates have been incorporated in an ethyl cellulose topical patch to treat pressure-induced diabetic ulcers.[130] Encapsulation of DFO within reverse micelles resulted in sustained release *in vitro*, and hypoxia-inducible factor-1 alpha (HIF-1α) stabilization occurred in a dose-dependent manner *in vivo*. Transdermal DFO was found to increase the rate of wound closure, dermal thickness, and VEGF expression, while promoting vascularization in mice. Additionally, when employed prophylactically, this transdermal DFO formulation treatment prevented ulcer formation in a mouse model. Mechanistically, DFO restores the HIF-1α activity that is diminished in diabetic patients by preventing oxidative stress. Reverse micelle technology has also been employed to evaluate the effects of DFO treatment on outcome in an *in vivo* model of breast reconstruction after radiation.[131] In a follow-up study, Duscher et al. reported an enhanced transdermal DFO formulation that employed reverse micelle encapsulation but eliminated plasticizers, emulsifiers, and surfactants that were not compatible with FDA regulations.[132] The enhanced formulation also had increased surface area for drug release due to its microtextured surface and facilitated accelerated wound healing in a mouse model compared to DFO drip-on and DFO spray, as well as the original formulation. Interestingly, diabetic wounds treated with the enhanced transdermal formulation also demonstrated improved biomechanical properties compared to other methods of DFO administration. Similarly, transferosomes loaded with DFO have been investigated for their efficacy in treating pressure ulcers. Transferosomes composed of soybean phosphatidylcholine (SPC) and surfactant at variable SPC amounts and ratios were optimized in a factorial study to tune entrapment efficiency, particle size, ζ potential, and *in vitro* drug release.[133] The most successful formulation was studied *in vivo*, and transferosome-loaded gels more effectively reduced wound area and increased collagen deposition and neovascularization in streptozotocin-induced diabetic rats compared to DFO solution-loaded gels and plain gels. Lecithin-based nanoparticles have yielded similar results in treating cutaneous wounds *in vivo* compared to simpler DFO formulations,[134] and topical lecithin-based nanoparticle formulations containing DFO have also been used to

promote microvascular regeneration and repair during airway transplant surgical procedures *in vivo*.[135]

IN VIVO CLEARANCE MECHANISMS AND DRUG ELIMINATION

IN formulations must not only overcome physiological barriers to brain targeting such as MCC and enzymatic degradation but should also be degradable and readily eliminated from the brain via the glymphatic system. Briefly, the glymphatic system eliminates macroscopic waste such as soluble metabolites and proteins via a series of perivascular tunnels and the interchange of cerebrospinal fluid (CSF) and interstitial fluid (ISF).[136,137] CSF influx in awake mice was reduced by 90% compared to unconscious mice when measured *in vivo* by 2-photon imaging, thus suggesting that the glymphatic system is active during sleep and that the primary biological function of sleep is neurotoxic waste clearance as opposed to rest.[136,138] For a full review of the glymphatic system and its physiology, see Jessen et al.[136] In addition to the glymphatic system, efflux transporters are also critical in expelling drugs and toxic metabolites from the brain. Such proteins belong to the ATP binding cassette (ABC) family and are capable of pumping a wide range of lipophilic substrates that have diffused into the cells composing the BBB back into the blood via the hydrolysis of ATP.[139–143] Several efflux transporters exist in the BBB, the most common of which are *p*-glycoprotein, breast cancer resistance protein, and the multidrug resistance-associated protein family.[139–143] While efflux transporters protect the brain from harmful chemical species in circulation, they also contribute to pharmacoresistance and make many CNS disorders difficult to treat.[139–143] These transporters influence not only elimination but also drug distribution to the CNS, and a better understanding of their substrate scope could lead to the development of more effective DFO nanoformulations for treating AD, PD, and ICH.

Though no biodegradable IN DFO delivery systems have been reported to date, biodegradable mucoadhesive particulates and microspheres have been studied. Spherical polymeric starch microspheres cross-linked with epichlorhydrine demonstrated an *in vitro* release rate of 73.11–86.21% and displayed good mucoadhesive properties and swelling.[144] Dry powder degradable starch microspheres of 45 μm diameter have been used to deliver IN insulin in rat models, where peak insulin concentration was reached within 8 min of dosing at 30% bioavailability.[145] Holmberg et al. reports that inhalation of 10 mg of degradable starch microspheres by a healthy adult once daily for 8 days does not alter MCC or nasal cavity geometry, thus indicating that starch microspheres do not adversely affect MCC or mucosa congestion.[146]

CONCLUSIONS AND FUTURE DIRECTIONS

The neuroprotective effects of the hexadentate iron chelator DFO in animal models of AD, PD, and secondary injury following ICH are strongly supported by abundant preclinical evidence. When administered to animal models of the aforementioned disease states either IN, systemically, or IP, DFO consistently improves behavioral outcome and alleviates oxidative stress (Figure 1) For AD, IN administered DFO has been consistently efficacious in multiple animal models, while systemically administered DFO has yielded mixed results in preclinical studies. IN administration of DFO has been more thoroughly

characterized compared to systemically administered DFO in animal models and thus provides a more direct route toward clinical implementation in the immediate future. In the way of PD, numerous efficacious IP formulations have been presented, though this route of administration is not frequently employed in treating humans. Both IN administered DFO and complex systemic nanoformulations of DFO show promise in treating PD, though the limited availability of such preclinical studies makes it difficult to predict which route may be translated more rapidly. Lastly, in the case of ICH, systemically administered DFO has been evaluated both preclinically and clinically, though many of these studies did not advance chelation therapy toward routine clinical implementation. Though IN formulations of DFO are few in number, they merit further exploration as a promising method to facilitate translation, as do complex nanoformulations designed for treating secondary injuries following ICH. Overall, IN administration of DFO appears promising in treating CNS disorders, as do many complex systemic nanoformulations designed to permeate the BBB. However, tremendous variation is observed in the dosing regimens employed in DFO treatment, and little data exists regarding the quantity of DFO that reaches the brain following administration, and these parameters should be more thoroughly characterized prior to clinical testing.

Though promising clinical trials indicate the potential of chelation therapy in treating neurodegeneration, the non-specific toxicity of DFO when administered systemically at high doses and the intensive regimen of parenteral injections result in low patient compliance and, in some cases, the occurrence of serious adverse events. As is the case for preclinical studies, significant variations in maximum tolerable dose are observed in clinical studies, and consistent dosing regimens remain elusive. Further studies should confirm the amount of DFO that reaches the brain when administered by various routes in the clinic.

IN administration of DFO offers offers promise in increasing patient compliance as this route is noninvasive and avoids systemic toxicity. More complex formulations (Figure 2) may lead to increased efficacy in treatment compared to traditional saline vehicles as these formulations protect against MCC and degradation by enzymes in the nasal mucosa. Alternatively, systemic formulations designed to prolong circulation time and decrease the minimum therapeutic dose may also prove useful in clinical application. Finally, the fate of the chelates resulting from successful DFO treatment in the brain has not been well characterized. It is possible that such chelates may cause chronic toxicity if not eliminated by efflux across the BBB or via the glymphatic system, so further study of their elimination is merited. Biodegradable IN and systemic formulations of DFO are thus of great clinical interest and merit further exploration for treating neurodegenerative disease.

ACKNOWLEDGMENTS

This work was funded in part by NIH grant R01DK099596.

ABBREVIATIONS

DFO	deferoxamine
IO	iron overload

ROS	reactive oxygen species
BBB	blood–brain barrier
CNS	central nervous system
IN	intranasal
MCC	mucocilliary clearance
IV	intravenous
IM	intramuscular
IP	intraperitoneal
SC	subcutaneous
AD	Alzheimer's disease
SP	senile plaques
PD	Parkinson's disease
ICH	intracerebral hemorrhage
RBCs	red blood cells
SN	substantia nigra

REFERENCES

(1). Hatcher HC; Singh RN; Torti FM; Torti SV Synthetic and natural iron chelators: therapeutic potential and clinical use. Future Med. Chem. 2009, 1 (9), 1643–70. [PubMed: 21425984]

(2). Kalinowski DS; Richardson D. R. J. P. r. The evolution of iron chelators for the treatment of iron overload disease and cancer. Pharmacol. Rev. 2005, 57 (4), 547–583. [PubMed: 16382108]

(3). Liu ZD; Hider RC Design of clinically useful iron (III)-selective chelators. Med. Res. Rev. 2002, 22 (1), 26–64. [PubMed: 11746175]

(4). Richardson DR; Ponka P. The molecular mechanisms of the metabolism and transport of iron in normal and neoplastic cells. Biochim. Biophys. Acta, Rev. Biomembr. 1997, 1331 (1), 1–40.

(5). Albretsen J. The toxicity of iron, an essential element. Veterinary Medicine 2006, 101 (2), 82.

(6). Kohgo Y; Ikuta K; Ohtake T; Torimoto Y; Kato J. Body iron metabolism and pathophysiology of iron overload. Int. J. Hematol. 2008, 88 (1), 7–15. [PubMed: 18594779]

(7). Di Nicola M; Barteselli G; Dell'Arti L; Ratiglia R; Viola F. Functional and structural abnormalities in deferoxamine retinopathy: a review of the literature. BioMed Res. Int. 2015, 2015, 1.

(8). Bayanzay K; Alzoebie L. Reducing the iron burden and improving survival in transfusion-dependent thalassemia patients: current perspectives. J. Blood Med. 2016, 7, 159. [PubMed: 27540317]

(9). Brittenham GM Iron-chelating therapy for transfusional iron overload. N. Engl. J. Med. 2011, 364 (2), 146–156. [PubMed: 21226580]

(10). Porter JB Deferoxamine pharmacokinetics. Semin. Hematol. 2001, 38 (1), 63–68. [PubMed: 11206963]

(11). Liu Z; Qiao J; Nagy T; Xiong MP ROS-triggered degradable iron-chelating nanogels: Safely improving iron elimination in vivo. J. Controlled Release 2018, 283, 84–93.

(12). Liu Z; Wang Y; Purro M; Xiong MP Oxidation-induced degradable nanogels for iron chelation. Sci. Rep. 2016, 6, 20923. [PubMed: 26868174]

(13). Liu Z; Lin T-M; Purro M; Xiong MP Enzymatically Biodegradable Polyrotaxane–Deferoxamine Conjugates for Iron Chelation.ACS Appl. Mater. Interfaces 2016, 8 (39), 25788–25797. [PubMed: 27623539]

(14). Ward RJ; Dexter D; Florence A; Aouad F; Hider R; Jenner P; Crichton RR Brain iron in the ferrocene-loaded rat: its chelation and influence on dopamine metabolism. Biochem. Pharmacol. 1995, 49 (12), 1821–1826. [PubMed: 7598744]

(15). Shachar DB; Kahana N; Kampel V; Warshawsky A; Youdim MB Neuroprotection by a novel brain permeable iron chelator, VK-28, against 6-hydroxydopamine lession in rats. Neuropharmacology 2004, 46 (2), 254–263. [PubMed: 14680763]

(16). Gordon GS; Ambruso DR; Robinson WA; Githens JH Intranasal administration of deferoxamine to iron overloaded patients. Am. J. Med. Sci. 1989, 297 (5), 280–284. [PubMed: 2640419]

(17). Hilditch-Maguire P; Trettel F; Passani LA; Auerbach A; Persichetti F; MacDonald ME Huntingtin: an iron-regulated protein essential for normal nuclear and perinuclear organelles. Human molecular genetics 2000, 9 (19), 2789–2797. [PubMed: 11092755]

(18). Niu L; Ye C; Sun Y; Peng T; Yang S; Wang W; Li H. Mutant huntingtin induces iron overload via up-regulating IRP1 in Huntington's disease. Cell Biosci. 2018, 8 (1), 41. [PubMed: 30002810]

(19). Hadzhieva M; Kirches E; Wilisch-Neumann A; Pachow D; Wallesch M; Schoenfeld P; Paege I; Vielhaber S; Petri S; Keilhoff G; Mawrin C. Dysregulation of iron protein expression in the G93A model of amyotrophic lateral sclerosis. Neuroscience 2013, 230, 94–101. [PubMed: 23178912]

(20). Lee JK; Shin JH; Gwag BJ; Choi E-J Iron accumulation promotes TACE-mediated TNF-α secretion and neurodegeneration in a mouse model of ALS. Neurobiol. Dis. 2015, 80, 63–69. [PubMed: 26002422]

(21). Chen J; Marks E; Lai B; Zhang Z; Duce JA; Lam LQ; Volitakis I; Bush AI; Hersch S; Fox JH Iron accumulates in Huntington's disease neurons: protection by deferoxamine. PLoS One 2013, 8 (10), No. e77023.

(22). Ruigrok MJ; de Lange EC Emerging insights for translational pharmacokinetic and pharmacokinetic-pharmacodynamic studies: towards prediction of nose-to-brain transport in humans. AAPS J. 2015, 17 (3), 493–505. [PubMed: 25693488]

(23). Illum L. Nasal drug delivery—possibilities, problems and solutions. J. Controlled Release 2003, 87 (1–3), 187–198.

(24). Alexander A; Saraf S. Nose-to-brain drug delivery approach: A key to easily accessing the brain for the treatment of Alzheimer's disease. Neural Regener. Res. 2018, 13 (12), 2102.

(25). Crowe TP; Greenlee MHW; Kanthasamy AG; Hsu WH Mechanism of intranasal drug delivery directly to the brain. Life Sci. 2018, 195, 44–52. [PubMed: 29277310]

(26). Alexander A; Agrawal M; Chougule MB; Saraf S; Saraf S. Nose-to-brain drug delivery: an alternative approach for effective brain drug targeting. Nanopharmaceuticals 2020, 1, 175–200.

(27). Alexander A; Agrawal M; Uddin A; Siddique S; Shehata AM; Shaker MA; Rahman SAU; Abdul MIM; Shaker MA Recent expansions of novel strategies towards the drug targeting into the brain. Int. J. Nanomed. 2019, 14, 5895.

(28). Lochhead JJ; Thorne RG Intranasal delivery of biologics to the central nervous system. Adv. Drug Delivery Rev. 2012, 64 (7), 614–628.

(29). Gänger S; Schindowski K. Tailoring formulations for intranasal nose-to-brain delivery: A review on architecture, physicochemical characteristics and mucociliary clearance of the nasal olfactory mucosa. Pharmaceutics 2018, 10 (3), 116.

(30). Gizurarson S. Anatomical and histological factors affecting intranasal drug and vaccine delivery. Curr. Drug Delivery 2012, 9(6), 566–582.

(31). Dhuria SV; Hanson LR; Frey WH II Intranasal delivery to the central nervous system: mechanisms and experimental considerations. J. Pharm. Sci. 2010, 99 (4), 1654–1673. [PubMed: 19877171]

(32). Battaglia L; Panciani PP; Muntoni E; Capucchio MT; Biasibetti E; De Bonis P; Mioletti S; Fontanella M; Swaminathan S. Lipid nanoparticles for intranasal administration: application to nose-to-brain delivery. Expert Opin. Drug Delivery 2018, 15 (4), 369–378.

(33). Furubayashi T; Kamaguchi A; Kawaharada K; Masaoka Y; Kataoka M; Yamashita S; Higashi Y; Sakane T. Evaluation of the contribution of the nasal cavity and gastrointestinal tract to drug absorption following nasal application to rats. Biol. Pharm. Bull. 2007, 30 (3), 608–611. [PubMed: 17329868]

(34). Pires A; Fortuna A; Alves G; Falcão A. Intranasal drug delivery: how, why and what for? J. Pharm. Pharm. Sci. 2009, 12 (3), 288–311. [PubMed: 20067706]

(35). Ikonomovic M; Klunk W; Abrahamson E; Wuu J; Mathis C; Scheff S; Mufson E; DeKosky S. Precuneus amyloid burden is associated with reduced cholinergic activity in Alzheimer disease. Neurology 2011, 77 (1), 39–47. [PubMed: 21700583]

(36). Colvez A; Joel M-E; Ponton-Sanchez A; Royer A-C Health status and work burden of Alzheimer patients'informal caregivers: comparisons of five different care programs in the European Union. Health Policy 2002, 60 (3), 219–233. [PubMed: 11965332]

(37). Liu J-L; Fan Y-G; Yang Z-S; Wang Z-Y; Guo C. Iron and Alzheimer's disease: from pathogenesis to therapeutic implications. Front. Neurosci. 2018, 12, 632. [PubMed: 30250423]

(38). Cheng X-S; Zhao K-P; Jiang X; Du L-L; Li X-H; Ma ZW; Yao J; Luo Y; Duan D-X; Wang J-Z; Zhou X-W Nmnat2 attenuates Tau phosphorylation through activation of PP2A.J. Alzheimer's Dis. 2013, 36 (1), 185–195. [PubMed: 23579329]

(39). Du L; Zhao Z; Cui A; Zhu Y; Zhang L; Liu J; Shi S; Fu C; Han X; Gao W; Song T; Xie L; Wang L; Sun S; Guo R; Ma G. Increased Iron Deposition on Brain Quantitative Susceptibility Mapping Correlates with Decreased Cognitive Function in Alzheimer's Disease.ACS Chem. Neurosci. 2018, 9 (7), 1849–1857.

(40). Lovell M; Robertson J; Teesdale W; Campbell J; Markesbery W. Copper, iron and zinc in Alzheimer's disease senile plaques. J. Neurol. Sci. 1998, 158 (1), 47–52. [PubMed: 9667777]

(41). van Bergen JMG; Li X; Quevenco FC; Gietl AF; Treyer V; Meyer R; Buck A; Kaufmann PA; Nitsch RM; van Zijl PCM; Hock C; Unschuld PG Simultaneous quantitative susceptibility mapping and Flutemetamol-PET suggests local correlation of iron and β-amyloid as an indicator of cognitive performance at high age. NeuroImage 2018, 174, 308–316. [PubMed: 29548847]

(42). Lane DJ; Ayton S; Bush AI Iron and Alzheimer's disease: an update on emerging mechanisms. J. Alzheimer's Dis. 2018, 64 (s1), S379–S395. [PubMed: 29865061]

(43). Boopathi S; Kolandaivel P. Fe2+ binding on amyloid β-peptide promotes aggregation. Proteins: Struct., Funct., Genet. 2016, 84 (9), 1257–1274. [PubMed: 27214008]

(44). Tahirbegi IB; Pardo WA; Alvira M; Mir M; Samitier J. Amyloid Aβ 42, a promoter of magnetite nanoparticle formation in Alzheimer's disease. Nanotechnology 2016, 27 (46), 465102.

(45). House E; Collingwood J; Khan A; Korchazkina O; Berthon G; Exley C. Aluminium, iron, zinc and copper influence the in vitro formation of amyloid fibrils of Aβ 42 in a manner which may have consequences for metal chelation therapy in Alzheimer's disease. J. Alzheimer's Dis. 2004, 6 (3), 291–301. [PubMed: 15201484]

(46). Smith MA; Harris PL; Sayre LM; Perry G. Iron accumulation in Alzheimer disease is a source of redox-generated free radicals. Proc. Natl. Acad. Sci. U. S. A. 1997, 94 (18), 9866–9868. [PubMed: 9275217]

(47). Zhang X-Y; Cao J-B; Zhang L-M; Li Y-F; Mi W-D Deferoxamine attenuates lipopolysaccharide-induced neuroinflammation and memory impairment in mice. J. Neuroinflammation 2015, 12, 20. [PubMed: 25644393]

(48). Guo C; Wang T; Zheng W; Shan Z-Y; Teng W-P; Wang Z-Y Intranasal deferoxamine reverses iron-induced memory deficits and inhibits amyloidogenic APP processing in a transgenic mouse model of Alzheimer's disease. Neurobiol. Aging 2013, 34 (2), 562–575. [PubMed: 22717236]

(49). Fine JM; Renner DB; Forsberg AC; Cameron RA; Galick BT; Le C; Conway PM; Stroebel BM; Frey WH; Hanson LR Intranasal deferoxamine engages multiple pathways to decrease memory loss in the APP/PS1 model of amyloid accumulation. Neurosci. Lett. 2015, 584, 362–367. [PubMed: 25445365]

(50). Guo C; Wang P; Zhong M-L; Wang T; Huang X-S; Li J-Y; Wang Z-Y Deferoxamine inhibits iron induced hippocampal tau phosphorylation in the Alzheimer transgenic mouse brain. Neurochem. Int. 2013, 62 (2), 165–172. [PubMed: 23262393]

(51). Guo C; Zhang Y-X; Wang T; Zhong M-L; Yang Z-H; Hao L-J; Chai R; Zhang S. Intranasal deferoxamine attenuates synapse loss via up-regulating the P38/HIF-1α pathway on the brain of APP/PS1 transgenic mice. Front. Aging Neurosci. 2015, 7, 104. [PubMed: 26082716]

(52). Zaman K; Ryu H; Hall D; O'Donovan K; Lin K-I; Miller MP; Marquis JC; Baraban JM; Semenza GL; Ratan RR Protection from oxidative stress–induced apoptosis in cortical neuronal cultures by iron chelators is associated with enhanced dna binding of hypoxia-inducible factor-1 and atf-1/creb and increased expression of glycolytic enzymes, p21waf1/cip1, and erythropoietin. J. Neurosci. 1999, 19 (22), 9821–9830. [PubMed: 10559391]

(53). Jaakkola P; Mole DR; Tian Y-M; Wilson MI; Gielbert J; Gaskell SJ; Kriegsheim A. v.; Hebestreit HF; Mukherji M; Schofield CJ; Maxwell PH; Pugh CW; Ratcliffe PJ Targeting of HIF-α to the von Hippel-Lindau ubiquitylation complex by O2-regulated prolyl hydroxylation. Science 2001, 292 (5516), 468–472. [PubMed: 11292861]

(54). Epstein ACR; Gleadle JM; McNeill LA; Hewitson KS; O'Rourke J; Mole DR; Mukherji M; Metzen E; Wilson MI; Dhanda A; Tian Y-M; Masson N; Hamilton DL; Jaakkola P; Barstead R; Hodgkin J; Maxwell PH; Pugh CW; Schofield CJ; Ratcliffe PJC elegans EGL-9 and mammalian homologs define a family of dioxygenases that regulate HIF by prolyl hydroxylation. Cell 2001, 107 (1), 43–54. [PubMed: 11595184]

(55). Fine JM; Baillargeon AM; Renner DB; Hoerster NS; Tokarev J; Colton S; Pelleg A; Andrews A; Sparley KA; Krogh KM; Frey WH; Hanson LR Intranasal deferoxamine improves performance in radial arm water maze, stabilizes HIF-1α, and phosphorylates GSK3β in P301L tau transgenic mice. Exp. Brain Res. 2012, 219 (3), 381–390. [PubMed: 22547371]

(56). Fine JM; Forsberg AC; Stroebel BM; Faltesek KA; Verden DR; Hamel KA; Raney EB; Crow JM; Haase LR; Knutzen KE; Kaczmarczek KD; Frey WH; Hanson LR Intranasal deferoxamine affects memory loss, oxidation, and the insulin pathway in the streptozotocin rat model of Alzheimer's disease. J. Neurol. Sci. 2017, 380, 164–171. [PubMed: 28870559]

(57). Hanson LR; Fine JM; Renner DB; Svitak AL; Burns RB; Nguyen TM; Tuttle NJ; Marti DL; Panter SS; Frey WH Intranasal delivery of deferoxamine reduces spatial memory loss in APP/PS1 mice. Drug Delivery Transl. Res. 2012, 2 (3), 160–168.

(58). Savory J; Exley C; Forbes WF; Huang Y; Joshi JG; Kruck T; Mclachlan DR; Wakayama I. Can the controversy of the role of aluminum in Alzheimer's disease be resolved? What are the suggested approaches to this controversy and methodological issues to be considered? J. Toxicol. Environ. Health 1996, 48 (6), 615–636. [PubMed: 8772802]

(59). Savory J; Huang Y; Wills M; Herman M. Reversal by desferrioxamine of tau protein aggregates following two days of treatment in aluminum-induced neurofibrillary degeneration in rabbit: implications for clinical trials in Alzheimer's disease. Neurotoxicology 1998, 19 (2), 209–214. [PubMed: 9553957]

(60). Esparza JL; Garcia T; Gómez M; Nogués MR; Giralt M; Domingo JL Role of deferoxamine on enzymatic stress markers in an animal model of Alzheimer's disease after chronic aluminum exposure. Biol. Trace Elem. Res. 2011, 141 (1–3), 232–245. [PubMed: 20455029]

(61). Agrawal M; Saraf S; Saraf S; Antimisiaris SG; Chougule MB; Shoyele SA; Alexander A. Nose-to-brain drug delivery: An update on clinical challenges and progress towards approval of anti-Alzheimer drugs. J. Controlled Release 2018, 281, 139–177.

(62). McLachlan DC; Kruck T; Kalow W; Andrews D; Dalton A; Bell M; Smith W. Intramuscular desferrioxamine in patients with Alzheimer's disease. Lancet 1991, 337 (8753), 1304–1308. [PubMed: 1674295]

(63). Kruck TP; Fisher EA; McLachlan DR A predictor for side effects in patients with Alzheimer's disease treated with deferoxamine mesylate. Clin. Pharmacol. Ther. 1993, 53 (1), 30–37. [PubMed: 8422739]

(64). McLachlan D; Smith W; Kruck T. Desferrioxamine and Alzheimer's disease: video home behavior assessment of clinical course and measures of brain aluminum. Ther. Drug Monit. 1993, 15 (6), 602–607. [PubMed: 8122302]

(65). Xu H; Wang Y; Song N; Wang J; Jiang H; Xie J. New Progress on the Role of Glia in Iron Metabolism and Iron-Induced Degeneration of Dopamine Neurons in Parkinson's Disease. Front. Mol. Neurosci. 2018, 10, 455. [PubMed: 29403352]

(66). Wang J; Xu H-M; Yang H-D; Du X-X; Jiang H; Xie J-X Rg1 reduces nigral iron levels of MPTP-treated C57BL6 mice by regulating certain iron transport proteins. Neurochem. Int. 2009, 54 (1), 43–48. [PubMed: 19000728]

(67). Zecca L; Berg D; Arzberger T; Ruprecht P; Rausch WD; Musicco M; Tampellini D; Riederer P; Gerlach M; Becker G. In vivo detection of iron and neuromelanin by transcranial sonography: a new approach for early detection of substantia nigra damage. Mov. Disord. 2005, 20 (10), 1278–1285. [PubMed: 15986424]

(68). Berg D. In vivo detection of iron and neuromelanin by transcranial sonography–a new approach for early detection of substantia nigra damage. Journal of neural transmission 2006, 113 (6), 775–780. [PubMed: 16755382]

(69). Dexter D; Wells F; Agid F; Agid Y; Lees A; Jenner P; Marsden C. Increased nigral iron content in postmortem parkinsonian brain. Lancet 1987, 330 (8569), 1219–1220.

(70). Oakley A; Collingwood J; Dobson J; Love G; Perrott H; Edwardson J; Elstner M; Morris C. Individual dopaminergicneurons show raised iron levels in Parkinson disease. Neurology 2007, 68 (21), 1820–1825. [PubMed: 17515544]

(71). Song N; Wang J; Jiang H; Xie J. Ferroportin 1 but not hephaestin contributes to iron accumulation in a cell model of Parkinson's disease.Free Radical Biol. Med. 2010, 48 (2), 332–341. [PubMed: 19913091]

(72). Fine JM; Forsberg AC; Renner DB; Faltesek KA; Mohan KG; Wong JC; Arneson LC; Crow JM; Frey WH; Hanson LR Intranasally-administered deferoxamine mitigates toxicity of 6-OHDA in a rat model of Parkinson's disease. Brain Res. 2014, 1574, 96–104. [PubMed: 24928620]

(73). Guo C; Hao L-J; Yang Z-H; Chai R; Zhang S; Gu Y; Gao H-L; Zhong M-L; Wang T; Li J-Y; Wang Z-Y Deferoxamine-mediated up-regulation of HIF-1αprevents dopaminergic neuronal death via the activation of MAPK family proteins in MPTP-treated mice. Exp. Neurol. 2016, 280, 13–23. [PubMed: 26996132]

(74). Febbraro F; Andersen KJ; Sanchez-Guajardo V; Tentillier N; Romero-Ramos M. Chronic intranasal deferoxamine ameliorates motor defects and pathology in the α-synuclein rAAV Parkinson's model. Exp. Neurol. 2013, 247, 45–58. [PubMed: 23531432]

(75). Dexter DT; Statton SA; Whitmore C; Freinbichler W; Weinberger P; Tipton KF; Della Corte L; Ward RJ; Crichton RR Clinically available iron chelators induce neuroprotection in the 6-OHDA model of Parkinson's disease after peripheral administration. Journal of Neural Transmission 2011, 118 (2), 223–231. [PubMed: 21165659]

(76). Xiong P; Chen X; Guo C; Zhang N; Ma B. Baicalin and deferoxamine alleviate iron accumulation in different brain regions of Parkinson's disease rats. Neural Regeneration Research 2012, 7 (27), 2092. [PubMed: 25558221]

(77). Haleagrahara N; Siew CJ; Ponnusamy K. Effect of quercetin and desferrioxamine on 6-hydroxydopamine (6-OHDA) induced neurotoxicity in striatum of rats. J. Toxicol. Sci. 2013, 38 (1), 25–33. [PubMed: 23358137]

(78). Lv H; Liu J; Wang L; Zhang H; Yu S; Li Z; Jiang F; Niu Y; Yuan J; Cui X; Wang W. Ameliorating effects of combined curcumin and desferrioxamine on 6-OHDA-induced rat mode of Parkinson's disease. Cell Biochem. Biophys. 2014, 70 (2), 1433–1438. [PubMed: 24989681]

(79). Anand P; Kunnumakkara AB; Newman RA; Aggarwal BB Bioavailability of curcumin: problems and promises. Mol. Pharmaceutics 2007, 4 (6), 807–818.

(80). Devos D; Moreau C; Kluza J; Laloux C; Petrault M; Devedjian J-C; Ryckewaert G; Garcon G; Rouaix N; Jissendi P; Dujardin K; Kreisler A; Simonin C; Destee A; Defebvre L; Marchetti P; Bordet R. Disease Modifying Strategy Based upon Iron Chelation in Parkinson's Disease: A Translational Study. Neurology 2012, 78, 240.

(81). Devos D; Moreau C; Devedjian JC; Kluza J; Petrault M; Laloux C; Jonneaux A; Ryckewaert G; Garcon G; Rouaix N; Duhamel A; Jissendi P; Dujardin K; Auger F; Ravasi L; Hopes L; Grolez G; Firdaus W; Sablonniere B; Strubi-Vuillaume I; Zahr N; Destee A; Corvol J-C; Poltl D; Leist

M; Rose C; Defebvre L; Marchetti P; Cabantchik ZI; Bordet R. Targeting chelatable iron as a therapeutic modality in Parkinson's disease. Antioxid. Redox Signaling 2014, 21 (2), 195–210.

(82). Grolez G; Moreau C; Sablonniere B; Garcon G; Devedjian J-C; Meguig S; Gele P; Delmaire C; Bordet R; Defebvre L; Cabantchik IZ; Devos D. Ceruloplasmin activity and iron chelation treatment of patients with Parkinson's disease. BMC Neurol. 2015, 15 (1), 74. [PubMed: 25943368]

(83). Martin-Bastida A; Ward RJ; Newbould R; Piccini P; Sharp D; Kabba C; Patel MC; Spino M; Connelly J; Tricta F; Crichton RR; Dexter DT Brain iron chelation by deferiprone in a phase 2 randomised double-blinded placebo controlled clinical trial in Parkinson's disease. Sci. Rep. 2017, 7 (1), 1398. [PubMed: 28469157]

(84). Qureshi AI; Mendelow AD; Hanley DF Intracerebral haemorrhage. Lancet 2009, 373 (9675), 1632–1644. [PubMed: 19427958]

(85). Wu H; Wu T; Xu X; Wang J; Wang J. Iron toxicity in mice with collagenase-induced intracerebral hemorrhage. J. Cereb. Blood Flow Metab. 2011, 31 (5), 1243–1250. [PubMed: 21102602]

(86). Sudlow C; Warlow C. Comparable studies of the incidence of stroke and its pathological types: results from an international collaboration. Stroke 1997, 28 (3), 491–499. [PubMed: 9056601]

(87). Wang X; Mori T; Sumii T; Lo EH Hemoglobin-induced cytotoxicity in rat cerebral cortical neurons: caspase activation and oxidative stress. Stroke 2002, 33 (7), 1882–1888. [PubMed: 12105370]

(88). Garton T; Keep RF; Hua Y; Xi G. Brain iron overload following intracranial haemorrhage. Stroke and Vascular Neurology 2016, 1 (4), 172–184. [PubMed: 28959481]

(89). Sadrzadeh S; Anderson DK; Panter SS; Hallaway P; Eaton J. Hemoglobin potentiates central nervous system damage. J. Clin. Invest. 1987, 79 (2), 662–664. [PubMed: 3027133]

(90). Xi G; Keep RF; Hoff JT Erythrocytes and delayed brain edema formation following intracerebral hemorrhage in rats. J. Neurosurg. 1998, 89 (6), 991–996. [PubMed: 9833826]

(91). Hanson LR; Roeytenberg A; Martinez PM; Coppes VG; Sweet DC; Rao RJ; Marti DL; Hoekman JD; Matthews RB; Frey WH; Panter SS Intranasal deferoxamine provides increased brain exposure and significant protection in rat ischemic stroke. J. Pharmacol. Exp. Ther. 2009, 330 (3), 679–686. [PubMed: 19509317]

(92). Cui H-J; He H.-y.; Yang A-L; Zhou H-J; Wang C; Luo J-K; Lin Y; Tang T. Efficacy of deferoxamine in animal models of intracerebral hemorrhage: a systematic review and stratified meta-analysis. PLoS One 2015, 10 (5), No. e0127256.

(93). Millán M; de la Ossa NP; Gasull T. Iron-Chelating Therapy in Stroke. In Metal Ion in Stroke; Li YV, Zhang JH, Eds.; Springer New York: New York, 2012; pp 283–301.

(94). Gu Y; Hua Y; Keep RF; Morgenstern LB; Xi G. Deferoxamine reduces intracerebral hematoma-induced iron accumulation and neuronal death in piglets. Stroke 2009, 40 (6), 2241–2243. [PubMed: 19372448]

(95). Xie Q; Gu Y; Hua Y; Liu W; Keep RF; Xi G. Deferoxamine attenuates white matter injury in a piglet intracerebral hemorrhage model. Stroke 2014, 45 (1), 290–292. [PubMed: 24172580]

(96). Degterev A; Huang Z; Boyce M; Li Y; Jagtap P; Mizushima N; Cuny GD; Mitchison TJ; Moskowitz MA; Yuan J. Chemical inhibitor of nonapoptotic cell death with therapeutic potential for ischemic brain injury. Nat. Chem. Biol. 2005, 1 (2), 112. [PubMed: 16408008]

(97). Zeng L; Tan L; Li H; Zhang Q; Li Y; Guo J. Deferoxamine therapy for intracerebral hemorrhage: A systematic review. PLoS One 2018, 13 (3), No. e0193615.

(98). Yu Y; Zhao W; Zhu C; Kong Z; Xu Y; Liu G; Gao X. The clinical effect of deferoxamine mesylate on edema after intracerebral hemorrhage. PLoS One 2015, 10 (4), No. e0122371.

(99). Selim M; Yeatts S; Goldstein JN; Gomes J; Greenberg S; Morgenstern LB; Schlaug G; Torbey M; Waldman B; Xi G; Palesch Y. Safety and tolerability of deferoxamine mesylate in patients with acute intracerebral hemorrhage. Stroke 2011, 42 (11), 3067–3074. [PubMed: 21868742]

(100). Suri MFK; Suarez JI; Rodrigue TC; Zaidat OO; Vazquez G; Wensel A; Selman WR Effect of treatment of elevated blood pressure on neurological deterioration in patients with acute intracerebral hemorrhage. Neurocrit. Care 2008, 9 (2), 177. [PubMed: 18506638]

(101). Yeatts SD; Palesch YY; Moy CS; Selim M. High Dose Deferoxamine in Intracerebral Hemorrhage (Hi-Def) Trial: Rationale, Design, and Methods. Neurocrit. Care 2013, 19 (2), 257–266. [PubMed: 23943316]

(102). Yu J; Yuan Q; Sun Y.-r.; Wu X; Du Z.-y.; Li Z.-q.; Wu X.-h.; Zhou L.-f.; Wu G; Hu J. Effects of deferoxamine mesylate on hematoma and perihematoma edema after traumatic intracerebral hemorrhage. Journal of Neurotrauma 2017, 34 (19), 2753–2759. [PubMed: 28462672]

(103). Selim M; Foster LD; Moy CS; Xi G; Hill MD; Morgenstern LB; Greenberg SM; James ML; Singh V; Clark WM; Norton C; Palesch YY; Yeatts SD; Dolan M; Yeh E; Sheth K; Kunze K; Muehlschlegel S; Nieto I; Claassen J; Falo C; Huang D; Beckwith A; Messe S; Yates M; O'Phelan K; Escobar A; Becker K; Tanzi P; Gonzales N; Tremont C; Venkatasubramanian C; Thiessen R; Save S; Verrault S; Collard K; DeGeorgia M; Cwiklinski V; Thompson B; Wasilewski L; Andrews C; Burfeind R; Torbey M; Hamed M; Butcher K; Sivakumar L; Varelas N; Mays-Wilson K; Leira E; Olalde H; Silliman S; Calhoun R; Dangayach N; Renvill R; Malhotra R; Kordesch K; Lord A; Calahan T; Geocadin R; Parish M; Frey J; Harrigan M; Leifer D; Mathias R; Schneck M; Bernier T; Gonzales-Arias S; Elysee J; Lopez G; Volgi J; Brown R; Jasak S; Phillips S; Jarrett J; Gomes J; McBride M; Aldrich F; Aldrich C; Kornbluth J; Bettle M; Goldstein J; Tirrell G; Shaw Q; Jonczak K. Deferoxamine mesylate in patients with intracerebral haemorrhage (i-DEF): a multicentre, randomised, placebo-controlled, double-blind phase 2 trial. Lancet Neurol. 2019, 18 (5), 428–438. [PubMed: 30898550]

(104). Wei G; Huang Y; Li F; Zeng F; Li Y; Deng R; Lai Y; Zhou J; Huang G; Chen D. Prescription of traditional Chinese medicine, prevents autophagy in experimental stroke by repressing p53-DRAM pathway.BMC Complementary Altern. Med. 2015, 15 (1), 377.

(105). Rassu G; Soddu E; Cossu M; Brundu A; Cerri G; Marchetti N; Ferraro L; Regan RF; Giunchedi P; Gavini E; Dalpiaz A. Solid microparticles based on chitosan or methyl-β-cyclodextrin: A first formulative approach to increase the nose-to-brain transport of deferoxamine mesylate. J. Controlled Release 2015, 201, 68–77.

(106). Challa R; Ahuja A; Ali J; Khar R. Cyclodextrins in drug delivery: an updated review.AAPS PharmSciTech 2005, 6 (2), E329–E357. [PubMed: 16353992]

(107). Sinha V; Singla AK; Wadhawan S; Kaushik R; Kumria R; Bansal K; Dhawan S. Chitosan microspheres as a potential carrier for drugs. Int. J. Pharm. 2004, 274 (1–2), 1–33. [PubMed: 15072779]

(108). Luppi B; Bigucci F; Corace G; Delucca A; Cerchiara T; Sorrenti M; Catenacci L; Di Pietra AM; Zecchi V. Albumin nanoparticles carrying cyclodextrins for nasal delivery of the anti-Alzheimer drug tacrine. Eur. J. Pharm. Sci. 2011, 44 (4), 559–565. [PubMed: 22009109]

(109). Buron G; Hacquemand R; Pourie G; Brand G. Inhalation exposure to acetone induces selective damage on olfactory neuroepithelium in mice. Neurotoxicology. NeuroToxicology 2009, 30, 114–120. [PubMed: 19071159]

(110). Agrawal M; Ajazuddin; Tripathi DK; Saraf S; Saraf S; Antimisiaris SG; Mourtas S; Hammarlund-Udenaes M; Alexander A. Recent advancements in liposomes targeting strategies to cross blood-brain barrier (BBB) for the treatment of Alzheimer's disease. J. Controlled Release 2017, 260, 61–77.

(111). Agrawal M; Saraf S; Saraf S; Antimisiaris SG; Hamano N; Li S-D; Chougule M; Shoyele SA; Gupta U; Ajazuddin; Alexander A. Recent advancements in the field of nanotechnology for the delivery of anti-Alzheimer drug in the brain region. Expert Opin. Drug Delivery 2018, 15 (6), 589–617.

(112). Elnaggar YS; Etman SM; Abdelmonsif DA; Abdallah OY Intranasal Piperine-Loaded Chitosan Nanoparticles as Brain-Targeted Therapy in Alzheimer's Disease: Optimization, Biological Efficacy, and Potential Toxicity. J. Pharm. Sci. 2015, 104 (10), 3544–3556.

(113). Zheng X; Shao X; Zhang C; Tan Y; Liu Q; Wan X; Zhang Q; Xu S; Jiang X. Intranasal H102 peptide-loaded liposomes for brain delivery to treat Alzheimer's disease. Pharm. Res. 2015, 32 (12), 3837–3849. [PubMed: 26113236]

(114). Zhang C; Chen J; Feng C; Shao X; Liu Q; Zhang Q; Pang Z; Jiang X. Intranasal nanoparticles of basic fibroblast growth factor for brain delivery to treat Alzheimer's disease. Int. J. Pharm. 2014, 461 (1–2), 192–202. [PubMed: 24300213]

(115). You L; Wang J; Liu T; Zhang Y; Han X; Wang T; Guo S; Dong T; Xu J; Anderson GJ; Liu Q; Chang Y-Z; Lou X; Nie G. Targeted Brain Delivery of Rabies Virus Glycoprotein 29-Modified Deferoxamine-Loaded Nanoparticles Reverses Functional Deficits in Parkinsonian Mice.ACS Nano 2018, 12 (5), 4123–4139. [PubMed: 29617109]

(116). Gotsbacher MP; Telfer TJ; Witting PK; Double KL; Finkelstein DI; Codd R. Analogues of desferrioxamine B designed to attenuate iron-mediated neurodegeneration: synthesis, characterisation and activity in the MPTP-mouse model of Parkinson's disease. Metallomics 2017, 9 (7), 852–864. [PubMed: 28466891]

(117). Liddell JR; Obando D; Liu J; Ganio G; Volitakis I; Mok SS; Crouch PJ; White AR; Codd R. Lipophilic adamantyl-or deferasirox-based conjugates of desferrioxamine B have enhanced neuroprotective capacity: implications for Parkinson disease. Free Radical Biol. Med. 2013, 60, 147–156. [PubMed: 23391576]

(118). Mursaleen L; Somavarapu S; Zariwala MG Deferoxamine and Curcumin Loaded Nanocarriers Protect Against Rotenone-Induced Neurotoxicity. J. Parkinson's Dis. 2020, 10 (1), 99–111. [PubMed: 31868679]

(119). Kulkarni AD; Vanjari YH; Sancheti KH; Belgamwar VS; Surana SJ; Pardeshi CV Nanotechnology-mediated nose to brain drug delivery for Parkinson's disease: a mini review. J. Drug Targeting 2015, 23 (9), 775–788.

(120). Acharya S; Meenambiga S. Nanotechnology in Parkinson's Disease-A Review. Res. J. Pharm. Technol. 2020, 13 (4), 1967–1971.

(121). Mavridis IN; Meliou M; Pyrgelis E-S; Agapiou E. Nanotechnology and Parkinson's disease. In Design of Nanostructures for Versatile Therapeutic Applications; Elsevier, 2018; pp 1–29.

(122). Wang N; Jin X; Guo D; Tong G; Zhu X. Iron chelation nanoparticles with delayed saturation as an effective therapy for Parkinson disease. Biomacromolecules 2017, 18 (2), 461–474. [PubMed: 27989126]

(123). Lundh B; Brockstedt U; Kristensson K. Lectin-binding pattern of neuroepithelial and respiratory epithelial cells in the mouse nasal cavity. Histochem. J. 1989, 21 (1), 33–43. [PubMed: 2745157]

(124). Wen Z; Yan Z; Hu K; Pang Z; Cheng X; Guo L; Zhang Q; Jiang X; Fang L; Lai R. Odorranalectin-conjugated nanoparticles: preparation, brain delivery and pharmacodynamic study on Parkinson's disease following intranasal administration. J. Controlled Release 2011, 151 (2), 131–138.

(125). Gao X; Wu B; Zhang Q; Chen J; Zhu J; Zhang W; Rong Z; Chen H; Jiang X. Brain delivery of vasoactive intestinal peptide enhanced with the nanoparticles conjugated with wheat germ agglutinin following intranasal administration. J. Controlled Release 2007, 121 (3), 156–167.

(126). Gao X; Tao W; Lu W; Zhang Q; Zhang Y; Jiang X; Fu S. Lectin-conjugated PEG–PLA nanoparticles: preparation and brain delivery after intranasal administration. Biomaterials 2006, 27 (18), 3482–3490. [PubMed: 16510178]

(127). Lavelle E; Grant G; Pusztai A; Pfüller U; O'Hagan D. Mucosal immunogenicity of plant lectins in mice. Immunology 2000, 99 (1), 30–37. [PubMed: 10651938]

(128). Dharmalingam P; Talakatta G; Mitra J; Wang H; Derry PJ; Nilewski LG; McHugh EA; Fabian RH; Mendoza K; Vasquez V; Hegde PM; Kakadiaris E; Roy T; Boldogh I; Hegde VL; Mitra S; Tour JM; Kent TA; Hegde ML Pervasive Genomic Damage in Experimental Intracerebral Hemorrhage: Therapeutic Potential of a Mechanistic-Based Carbon Nanoparticle. ACS Nano 2020, 14 (3), 2827–2846. [PubMed: 32049495]

(129). Jones G; Goswami SK; Kang H; Choi HS; Kim J. Combating iron overload: a case for deferoxamine-based nanochelators. Nanomedicine 2020, 15 (13), 1341.

(130). Duscher D; Neofytou E; Wong VW; Maan ZN; Rennert RC; Inayathullah M; Januszyk M; Rodrigues M; Malkovskiy AV; Whitmore AJ; Walmsley GG; Galvez MG; Whittam AJ; Brownlee M; Rajadas J; Gurtner GC Transdermal deferoxamine prevents pressure-induced diabetic ulcers. Proc. Natl. Acad. Sci. U. S. A. 2015, 112 (1), 94–99. [PubMed: 25535360]

(131). Snider AE; Lynn JV; Urlaub KM; Donneys A; Polyatskaya Y; Nelson NS; Ettinger RE; Gurtner GC; Banaszak Holl MM; Buchman SR Topical deferoxamine alleviates skin injury and normalizes atomic force microscopy patterns following radiation in a murine breast reconstruction model. Ann. Plast. Surg. 2018, 81 (5), 604. [PubMed: 30113984]

(132). Duscher D; Trotsyuk AA; Maan ZN; Kwon SH; Rodrigues M; Engel K; Stern-Buchbinder ZA; Bonham CA; Barrera J; Whittam AJ; Hu MS; Inayathullah M; Rajadas J; Gurtner GC Optimization of transdermal deferoxamine leads to enhanced efficacy in healing skin wounds. J. Controlled Release 2019, 308, 232–239.

(133). El-Gizawy SA; Nouh A; Saber S; Kira AY Deferoxamine-loaded transfersomes accelerates healing of pressure ulcers in streptozotocin-induced diabetic rats.J. Drug Delivery Sci. Technol. 2020, 58, 101732.

(134). Qayoom A; Aneesha V; Anagha S; Dar JA; Kumar P; Kumar D. Lecithin-based deferoxamine nanoparticles accelerated cutaneous wound healing in diabetic rats. Eur. J. Pharmacol. 2019, 858, 172478.

(135). Jiang X; Malkovskiy AV; Tian W; Sung YK; Sun W; Hsu JL; Manickam S; Wagh D; Joubert L-M; Semenza GL; Rajadas J; Nicolls MR Promotion of airway anastomotic microvascular regeneration and alleviation of airway ischemia by deferoxamine nanoparticles. Biomaterials 2014, 35 (2), 803–813. [PubMed: 24161166]

(136). Jessen NA; Munk ASF; Lundgaard I; Nedergaard M. The glymphatic system: a beginner's guide. Neurochem. Res. 2015, 40 (12), 2583–2599. [PubMed: 25947369]

(137). Iliff JJ; Wang M; Liao Y; Plogg BA; Peng W; Gundersen GA; Benveniste H; Vates GE; Deane R; Goldman SA; Nagelhus EA; Nedergaard M. A paravascular pathway facilitates CSF flow through the brain parenchyma and the clearance of interstitial solutes, including amyloid β. Sci. Transl. Med. 2012, 4 (147), 147ra111–147ra111.

(138). Xie L; Kang H; Xu Q; Chen MJ; Liao Y; Thiyagarajan M; O'Donnell J; Christensen DJ; Nicholson C; Iliff JJ; Takano T; Deane R; Nedergaard M. Sleep drives metabolite clearance from the adult brain. Science 2013, 342 (6156), 373–377. [PubMed: 24136970]

(139). Sun H; Dai H; Shaik N; Elmquist WF Drug efflux transporters in the CNS. Adv. Drug Delivery Rev. 2003, 55 (1), 83–105.

(140). Löscher W; Potschka H. Blood-brain barrier active efflux transporters: ATP-binding cassette gene family. NeuroRx 2005, 2 (1), 86–98. [PubMed: 15717060]

(141). Mason WP Blood-brain barrier-associated efflux transporters: a significant but underappreciated obstacle to drug development in glioblastoma. Neuro Oncology 2015, 17 (9), 1181–1182. [PubMed: 26138634]

(142). Qosa H; Miller DS; Pasinelli P; Trotti D. Regulation of ABC efflux transporters at blood-brain barrier in health and neurological disorders. Brain Res. 2015, 1628, 298–316. [PubMed: 26187753]

(143). Schinkel AH; Jonker JW Mammalian drug efflux transporters of the ATP binding cassette (ABC) family: an overview. Adv. Drug Delivery Rev. 2012, 64, 138–153.

(144). Yadav A; Mote H. Development of biodegradable starch microspheres for intranasal delivery. Indian Journal of Pharmaceutical Sciences 2008, 70 (2), 170. [PubMed: 20046707]

(145). Björk E; Edman P. Degradable starch microspheres as a nasal delivery system for insulin. Int. J. Pharm. 1988, 47 (1–3), 233–238.

(146). Holmberg K; Bjork E; Bake B; Edman P. Influence of degradable starch microspheres on the human nasal mucosa. Rhinology 1994, 32 (2), 74–7. [PubMed: 7939145]

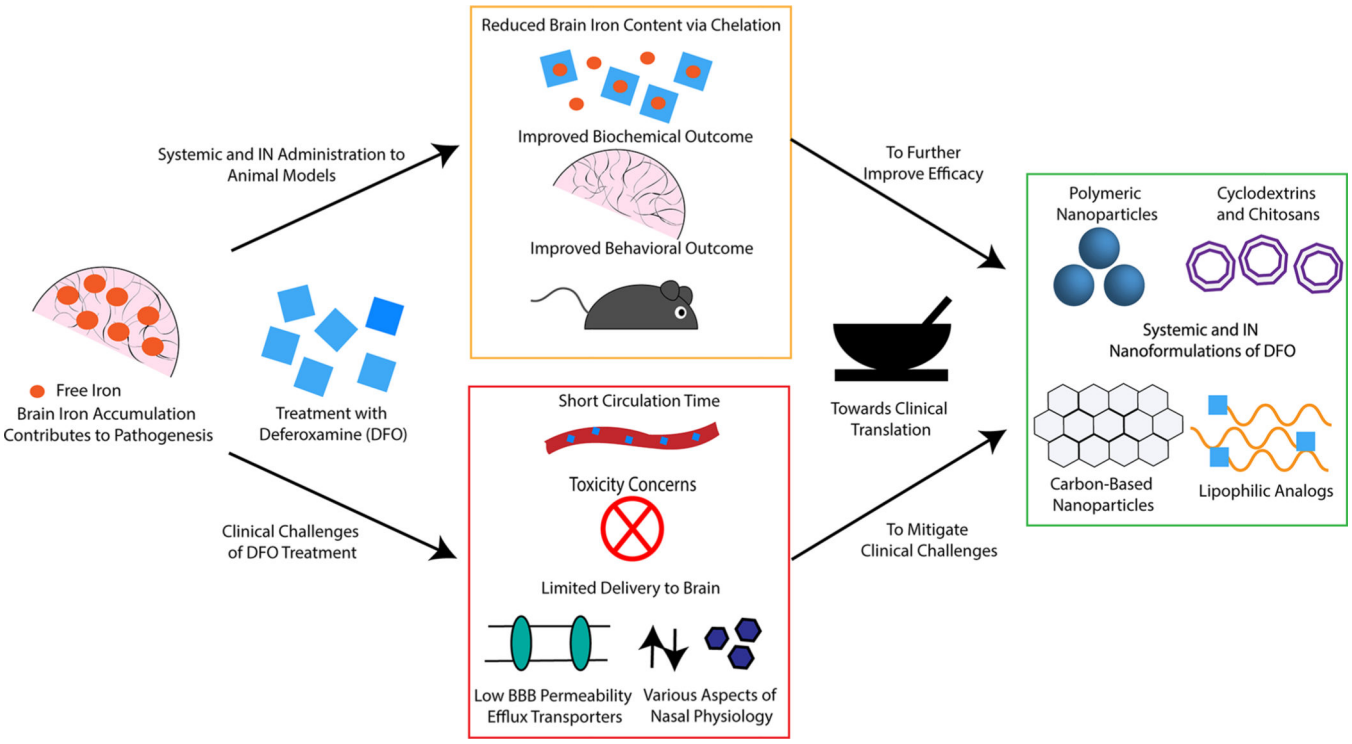

Figure 1.

Challenges and opportunities for deferoxamine delivery to treat Alzheimer's disease, Parkinson's disease, and secondary injury following intracerebral hemorrhage. Systemically and intranasally administered deferoxamine improves outcome in animal models, though deferoxamine administration has several clinical limitations. The use of nanoformulations of deferoxamine provides an avenue for clinical translation.

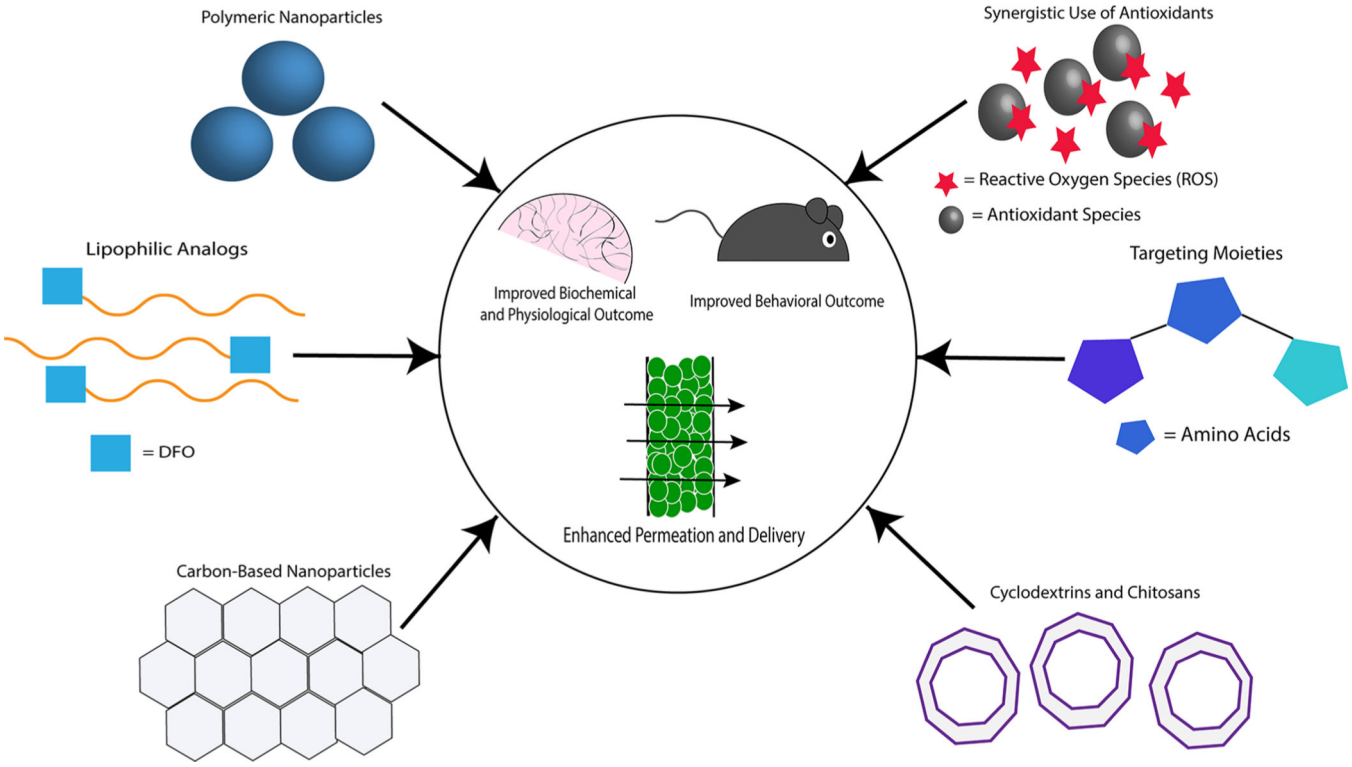

Figure 2.

Various strategies incorporated in systemic and intranasal nanoformulations of DFO to improve the efficacy of chelation therapy in treating Alzheimer's disease, Parkinson's disease, and secondary injury following intracerebral hemorrhage. Strategies such as the synergistic leverage of antioxidant species or targeting chemical moieties can be used in conjunction with delivery systems to ultimately improve biochemical, physiological, and behavioral outcomes in animal models.

Table 1.

Outcomes of IN DFO Treatment in Animal Models of AD at Various Doses and Dosing Intervals

source	animal model	formulation	dose administered	dose detected in brain	outcome
Guo etal.[48]	male APP/PS1 double transgenic mice watered with high-dose	IN saline solution	200 mg/kg bodyweight once every other day for 90 days		reduced expression and phosphorylation of APP protein; attenuated Aβ burden; improved memory retention
Fine etal.[49]	male APP/PS1 amyloid mice	10% DFO solution in 0.2X phosphate buffered saline (PBS) at pH 6.0 delivered IN	3X/week with 0.24C for 18 weeks from 36 to 54 weeks of age; dosing was continued through 4 weeks of behavioral testing beginning at week 54		decreased loss of reference and working memory in Morris and radial arm water mazes; decreased soluble Aβ40 and Aβ42 in cortex and hippocampus; decreased oxidative stress; decreased GSK3β activity
Guo etal.[50]	male APP/PS1 double transgenic mice	IN saline solution	200 mg/kg bodyweight once every other day for 90 days		decreased induced tau phosphorylation; decreases Fe-induced CDK5 activity and GSK3β activity
Guo etal.[51]	male APP/PS1 double transgenic mice	saline solution delivered IN	200 mg/kg once every other day for 3 months beginning at 6 months of age		decreased Aβ deposition; rescued synapse loss; upregulated HIF-la mRNA and protein, induced TFR, DMT1, and BDNF; decrease in iron in the hippocampus; enhanced phosphorylation of (MAPK)/P38 kinase
Fine etal.[55]	P301L transgenic tau mice	10% solution in 0.2X PBS at pH 6.0 delivered IN	2.4 mg 3X/week starting at 11 weeks of age; behavioral testing began at 32 weeks, and IN DFO treatment was continued through 5 weeks of behavioral testing		improved performance in radial arm water maze test when compared to untreated transgenic mice; increased pGSK3β and HIF-la in transgenic mice
Fine etal.[56]	male ICV STZ rat model (nonamyloid/ tau model)	10% solution in 0.2X PBS at pH 6.0 delivered IN	3 mg 3X/week for 4 weeks postsurgery; behavioral tests began at 4 weeks, and dosing was continued through such experiments; selected groups were pretreated with DFO for 4 days prior to surgery		ICV STZ rats treated with IN DFO both before and after surgery had shorter escape latencies in Morris water maze behavioral tests; pretreatment with IN DFO decreased foot slips on tapered balance beam test; IN DFO treatment decreased oxidation and increased insulin receptor expression
Hanson etal.[57]	male C57 mice for radiolabeled pharmacokinetic studies; male APP/PS1 mice	10% solution in 0.2X PBS at pH 6.0	2.4 mg 3X/week for 4 weeks beginning at 36 weeks of age	0.4–29 μM after 30 min	reduced escape latencies in Morris water maze; reduced brain levels of aluminum; no change in amyloid plaque deposition

Table 2.

Outcomes of Systemic DFO Treatment in Animal Models of AD at Various Doses and Dosing Intervals

source	animal model	formulation	dose administered	outcome
Savory etal.[59]	New Zealand white rabbits receiving intracisternal Injections of Al	IM DFO	given 2 days prior to sacrifice at 4, 6, or 8 days	DFO treatment reversed Al-induced neurofibrillary degeneration
Esparza etal.[60]	female AβPP transgenic mice orally exposed to Al	SC injections	0.20 mmol/kg/d twice per week for six months	DFO treatment does not appear to mitigate pro-oxidative events

Table 3.

Outcomes of Clinical Trials of DFO in AD Patients

source	formulation	dose administered	outcome
McLachlan et al.[62]	IM DFO	125 mg twice/day, 5 days/ week	DFO treatment reduced the decline in daily living skills compared to placebo and oral treatment

Table 4.

Outcomes of IN DFO Treatment in Animal Models of PD at Various Doses and Dosing Intervals

source	animal model	formulation	dose administered	outcome
Fine et al.[72]	male 6-hydroxydopamine (6-OHDA) rats	10% solution in 0.2X PBS at pH 6.0 delivered IN	3 mg IN DFO 2X/week for 4 weeks postsurgery; behavior testing began 5 weeks after surgery and dosing was continued through these studies; rats were pretreated 4 days, 2 days, and 30 min before surgery	reduced number of contralateral turns after injection of apomorphine HC1 in the apomorphine-induced rotational test; decreased limb asymmetry in the rearing tube when measured with contralateral limb touches; a slight decrease in the number of contralateral foot slips in tapered balance beam test; preservation of tyrosine hydroxylase immunoreactive neurons in substantia nigra
Guo et al.[73]	male C57BL/6 mice treated IP with 34 mg/kg of l-methyl-4-phenyl-1,2,3,6-tetrahydropyridine (MPTP) once a day for 5 days	IN 0.9% saline solution	200 mg/kg delivered IN once every other day for 4 weeks; treatment started after 5 days of MPTP treatment	increased survival of TH-positive neurons; decreased action of astrocytes in SN and striatum; up-regulated HIF-lα protein expression, TH, VEGF, and GAP43; down-regulated a-synuclein, DMT1, and TFR expression; inhibited MPTP-induced JNK phosphorylation; enhanced phosphorylation of extracellular regulated protein kinases and (MAPK)/P38 kinase
Febbraro et al.[74]	female Sprague—Dawley rats unilaterally injected in the midbrain with rAAV encoding α-synuclein	10% DFO solution in saline adjusted to pH 4.65	6 mg 3X/week for 3 or 7 weeks beginning 1 week after surgery	decrease in the number of pathological α-synuclein formations in striatal fibers; partial improvement in motor behavior in stepping and cylinder tests and amphetamine-induced rotations; treatment did not protect against dopaminergic cell death accompanying α-synuclein overexpression

Table 5.

Outcomes of Systemic DFO and IP DFO Treatment in Animal Models of PD at Various Doses and Dosing Intervals

source	animal model	formulation	dose administered	outcome
Dexter et al.[75]	male 6-OHDA Sprague—Dawley rats	0.9% saline delivered IP	30 mg/kg 2X/day I day prior to 6- OHDA lesion and for 4 days after	attenuated loss of striatal dopamine; attenuated the loss of dopaminergic neurons
Ward et al.[14]	male ferrocene-loaded Wistar rats	delivered IP	30 mg/kg 3X/week for 2 or 4 weeks after model induction	decrease in iron content in the SN, cerebellum, and cerebral cortex; reduced dopamine turnover and DOPAC
Xiong et al.[76]	male rotenone- induced PD Wistar rats	delivered IP	60 mg/kg/day for 8 weeks after model induction	inhibited iron accumulation in the SN, striatum globus pallidus, hippocampus, and cerebellum; reduced loss of TH- positive cells; protected dopaminergic neurons
Haleagrahara et al.[77]	male 6-OHDA Sprague—Dawley rats	delivered IP	50 mg/kg for 14 days beginning 48 h after surgery	significantly reversed decreases in striatal dopamine, glutathione (GSH), superoxide dismutase (SOD); significantly reversed the increase in protein carbonyl content (PCC); increased striatal neuronal number
Lv et al.[78]	male 6-OHDA Sprague—Dawley rats	delivered IP	50 mg/kg for 14 days beginning 48 h after surgery	attenuated loss of dopamine; decrease in PCC level; elevated GSH and SOD level; increased count of antioxidant enzymes

Table 6.

Outcomes of IN DFO Treatment in Animal Models of ICH at Various Doses and Dosing Intervals

source	animal model	formulation	dose administered	dose detected in brain	outcome
Hanson et al.[91]	MCAO maie Sprague—Dawley rats	10% solution of DFO in water delivered IN	rats were pretreated 3X at 3 h intervals 48 h before MCAO with either 6 mg doses or 1.8 mg doses; p re treatment with a single 6 mg dose was also tested; 6 mg dose administered immediately after reperfusion, at 2 h, and at 4 h; 24 h after MCAO rats were dosed 3X at 3 h intervals	0.9–18.5 μM after 30 min	55% decrease in infarct volume in both pre- and post-treated rats; a 200- fold increase of DFO in the cortex relative to blood compared to IV delivery; decrease in post-ischemic weight loss in pretreated rats

Table 7.

Nanoformulations of DFO for Treating AD, PD, and ICH[a]

source	animal model	formulation	dose administered	dose detected in brain	outcome
Rassu et al.[105]	male Wistar rats	chitosan chloride and methyl-β-cyclo dextrin microparticles encapsulating DFO produced by spray drying	200 μg DFO encapsulated in microparticles	3.83 ± 0.68 μg/mL for chitosan microparticles and 14.37 ± 1.69 μg/mL for methyl-β- cyclodextrin microparticles	encapsulation in microparticles increased uptake to the CSF 30 min aftei insufflation compared to DFO solution
You et al.[115]	male C57BL/6 MPTP mice	RVG29-mPEG—PLGA-DFO nanoparticles delivered IV	35 mg/kg once every other day for 12 days following MPTP injection		decreased iron content and oxidative stress levels in the SN and striatum; reduced dopaminergic neuron damage; reversed neurobehavioral deficits
Gotsbacher et al.[116]	male C57BL/6 MPTP mice	lipophilic conjugates of DFO delivered IP	40 μmol/kg/day beginning after the final MPTP injection for 21 days		lipophilic compounds showed average plasma protein binding 6X greater than DFO; ancillary fragments possessed antioxidant activity; selected compounds were neuroprotective
Dharmalineam et al.[128]	C57BL/6 mice	DEF-PEG-HCC in saline delivered IP	2 mg/kg 30 min after induced ICH		enhanced nuclear and mitochondrial genome fidelity and decrease in expression of senescence markers after 12 h

[a]Only nanoformulations that have been evaluated in preclinical models are tabulated.